Modeling the Mediterranean Sea interannual variability during 1961-2000: Focus on the Eastern Mediterranean Transient

J. Beuvier, F. Sevault, M. Herrmann, H. Kontoyiannis, W. Ludwig, M. Rixen, E. Stanev, K. Béranger, S. Somot

Modeling the Mediterranean Sea interannual variability during 1961–2000: Focus on the Eastern Mediterranean Transient

J. Beuvier,[1,2,3] F. Sevault,[1] M. Herrmann,[1] H. Kontoyiannis,[4] W. Ludwig,[5] M. Rixen,[6] E. Stanev,[7] K. Béranger,[2,3] and S. Somot[1]

Received 30 October 2009; revised 29 March 2010; accepted 8 April 2010; published 18 August 2010.

[1] This work is dedicated to the study of the climate variability of the Mediterranean Sea, in particular the study of the Eastern Mediterranean Transient (EMT) which occurred in the early 1990s. Simulations of the 1961–2000 period have been carried out with an eddy-permitting Ocean General Circulation Model of the Mediterranean Sea, driven by realistic interannual high-resolution air-sea fluxes. Using different databases for the river runoff, Black Sea inflow, and Atlantic thermohaline characteristics at climatological or interannual scales, we assess the effects of the non-atmospheric hydrological forcings on the simulation of the interannual variations of the Mediterranean circulation. The evolution of the basin-scale heat content is in very good agreement with the observations (especially in the surface and intermediate layers), while the agreement is lower for the evolution of the salt content. Convection events in the Aegean Sea are noticed in the simulations between 1972 and 1976, in the late 1980s, and around the EMT period. The formation rates of Cretan Deep Water (CDW) are different during these periods, allowing or preventing the spreading of CDW into the eastern Mediterranean. The sequence of the EMT events is well reproduced: the high winter oceanic surface cooling and net evaporation over the Aegean Sea in the early 1990s, the high amount of dense CDW formed during these winters, and then the overflow and the spreading of this CDW in the eastern Mediterranean. Among the preconditioning processes suggested in the literature, we find that changes in the Levantine surface circulation, possibly induced by the presence in the Cretan Passage of anticyclonic eddies and a lasting period with reduced net precipitation over the eastern Mediterranean, lead to an increase of the salt content of the Aegean Sea. Changes in the Black Sea freshwater inflow or in the characteristic of the Atlantic Water entering at the Gibraltar Strait also modify the thermohaline state of the Aegean Sea before the EMT. But, as none of these preconditioning factors has a lasting impact on lowering the vertical stratification of the Aegean Sea, we conclude that concerning the EMT, the major triggering elements are the atmospheric fluxes and winds occurring in winters 1991–1992 and 1992–1993.

Citation: Beuvier, J., F. Sevault, M. Herrmann, H. Kontoyiannis, W. Ludwig, M. Rixen, E. Stanev, K. Béranger, and S. Somot (2010), Modeling the Mediterranean Sea interannual variability during 1961–2000: Focus on the Eastern Mediterranean Transient, *J. Geophys. Res.*, *115*, C08017, doi:10.1029/2009JC005950.

1. Introduction

[2] The Mediterranean Sea circulation and water masses have been studied for a long time and schemes of the steady state of its thermohaline circulation have been proposed [*Wüst*, 1961; *Robinson et al.*, 2001]. The Atlantic Water (AW) enters the western Mediterranean at the Gibraltar Strait in the surface layer and flows towards the eastern Mediterranean in a cyclonic manner [*Millot*, 1999; *Hamad et al.*, 2005; *Alhammoud et al.*, 2005]. Deep winter convection forms dense waters sinking at different depths in the following four main areas (see Figure 1 for geographical locations): (1) the Levantine Intermediate Water (LIW) and sometimes the Levantine Deep Water (LDW) in the Levantine basin, mainly in the Rhodes gyre, (2) the Cretan

[1]Groupe d'Etude de l'Atmosphère Météorologique, Centre National de Recherches Météorologiques, Météo-France, CNRS, Toulouse, France.
[2]Unité de Mécanique, Ecole Nationale Supérieure de Techniques Avancées, ParisTech, Palaiseau, France.
[3]Laboratoire d'Océanographie et du Climat: Expérimentation et Approches Numériques, Institut Pierre Simon Laplace des Sciences de l'Environnement, Paris, France.
[4]Institute of Oceanography, Hellenic Center for Marine Research, Athens, Greece.
[5]Centre de Formation et de Recherche sur l'Environnement Marin, University of Perpignan, Perpignan, France.
[6]NATO Undersea Research Centre, La Spezia, Italy.
[7]Institute for Coastal Research, GKSS, Geesthacht, Germany.

0148-0227/10/2009JC005950

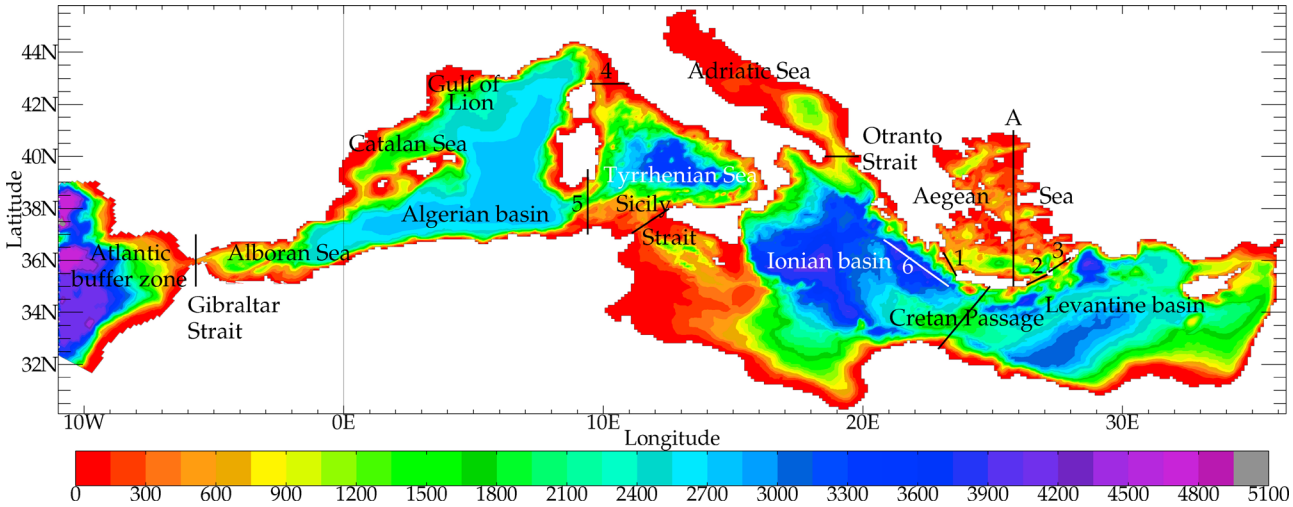

Figure 1. Bathymetry (in m) of NEMOMED8 in partial-step configuration and location of main Mediterranean basins, straits and places. 1: Antikithira Strait. 2: Kassos Strait. 3: Karpathos Strait. 4: Corsica Strait. 5: Sardinia Strait. 6: Hellenic Trench. A: location of the meridian sections of Figure 14.

Intermediate Water (CIW) and sometimes the Cretan Deep Water (CDW) in the southern part of the Aegean Sea (Cretan Sea), (3) the Adriatic Deep Water (ADW) in the Adriatic Sea, and (4) the Western Mediterranean Deep Water (WMDW) in the Gulf of Lions.

[3] The eastern Mediterranean deep layers are filled by Eastern Mediterranean Deep Water (EMDW) that typically originates in the Adriatic Sea (ADW) and in one exceptional case in the Cretan Sea (CDW). Shelf deep convection process is also present in specific locations along the northern boundary, i.e., in the Gulf of Lions [*Canals et al.*, 2006], in the North of Adriatic Sea [*Artegiani et al.*, 1997] and in the Aegean Sea [*Zervakis et al.*, 2000]. The intermediate waters mainly flow at a depth of about 300 to 500m from the northern Levantine basin or eastern Ionian basin towards the other sub-basins, namely the Adriatic Sea and the Gulf of Lions. The LIW also propagates northwards off the Turkish coasts in the Aegean Sea [*Gertman et al.*, 2006]. The deep waters are strongly constrained by Mediterranean straits and sills (Cretan Arc straits, Cretan Passage, Otranto, Sicily, Corsica and Sardinia straits), which limit the exchanges between the various sub-basins.

[4] This typical steady-state picture of the Mediterranean Thermohaline Circulation (MTHC hereafter), which was valid for almost the entire twentieth century and in which the EMDW was of Adriatic origin, was fundamentally disturbed by the discovery of the so-called Eastern Mediterranean Transient (EMT) during the 1990s, which was first reported by *Roether et al.* [1996]. Then, its evolution has been further analyzed by *Klein et al.* [1999], *Lascaratos et al.* [1999], *Theocharis et al.* [1999], *Zervakis et al.* [2004], and *Roether et al.* [2007]. Observational evidences proved that during the beginning of the 1990s, the EMDW was not formed anymore in the Adriatic Sea but in the Aegean Sea. Very dense waters were formed during several years within the Aegean Sea until they filled this small basin. This newly formed water mass then overflowed in the Levantine and Ionian basins through the Cretan Arc straits (Antikithira, Kassos and Karpathos straits). The densest water overflows have been recorded in the deepest straits of the Cretan Arc, Kassos and Karpathos, situated at the eastern part of Crete [*Theocharis et al.*, 2002; *Kontoyiannis et al.*, 2005]. Note that during the winter 1991–1992, LDW was also observed in the Rhodes gyre [*Sur et al.*, 1992], proving the exceptionality of this particular winter in terms of buoyancy loss. After overflowing the Cretan straits and despite the mixing due to lighter water mass entrainment, the newly formed water mass spreads towards the bottom of the eastern Mediterranean. The major part of the dense water vein turned westward driven by the Coriolis force and by the local topography represented by the Hellenic Trench, west of Crete. It then continued to flow along the continental slope in the Ionian basin [*Roether et al.*, 2007]. Under the sill of the Cretan Passage, i.e., below 2000 m, the rest of the vein flowed southwards in a cyclonic circulation in the Levantine basin. A part of the new EMDW also spreads directly and slowly eastwards in the Levantine basin, probably carried by mesoscale eddies.

[5] The new EMDW replaced and uplifted the old EMDW, creating a warm, salty and dense anomaly in the hydrographic characteristics of the deep layers of the eastern Mediterranean and a cold and fresh anomaly in those of the intermediate layers [*Theocharis et al.*, 2002; *Gasparini et al.*, 2005]. This transient phenomenon has even had an impact on the biogeochemistry of the eastern Mediterranean [*Klein et al.*, 2003]. Since 1998, a new phase of the EMT has been observed with warm and salty Cretan Intermediate Water (CIW) flowing out of the Aegean Sea through the Antikithira Strait. This CIW was observed in the Ionian basin at about 400–500 m depth around 1998–2000. They were situated above the old EMDW (of ADW origin) which were at about 1500 m depth and above the new EMDW (of CDW origin) which were at about 2500 m depth [*Theocharis et al.*, 2002; *Kontoyiannis et al.*, 2005]. Despite the lack of observations showing the detailed path of this CIW in the eastern Mediterranean, it may have passed through the Sicily Strait

around year 2000 [*Gasparini et al.*, 2005] and reached the western Mediterranean [*Schroeder et al.*, 2008]. The formation phase and the spreading phase of the new EMDW have been recently summarized by *Roether et al.* [2007]. Different hypotheses concerning the preconditioning of the EMT and its timing have been proposed in the literature, mainly based on the available observations. Among the preconditioning hypotheses and the potential triggering elements, we found the following: (1) a change in the surface circulation, which could have modified the AW path, preventing the AW flow towards the far eastern Mediterranean and isolating the Levantine basin and the Aegean Sea from a freshwater input [*Malanotte-Rizzoli et al.*, 1999; *Samuel et al.*, 1999; *Theocharis and Kontoyiannis*, 1999]; (2) the presence of three anticyclonic eddies south of Crete, which would have modified the LIW path towards the Aegean Sea and consequently increased the salt content of the Aegean Sea [*Malanotte-Rizzoli et al.*, 1999; *Samuel et al.*, 1999]; (3) the salinity increase of the deep waters observed during the end of the 1980s in the eastern Mediterranean can be explained, for 10 to 40% of it, by changes in the net surface evaporation but the major part of the change should have been driven by internal salinity redistribution [*Josey*, 2003]; (4) a decrease in the Black Sea freshwater input due to a reduction of the river runoff which flow into it [*Zervakis et al.*, 2000; *Stanev and Peneva*, 2002]; (5) the start of the intense winter convection in 1987 in the northern Aegean Sea [*Zervakis et al.*, 2000; *Gertman et al.*, 2006]; Cretan Deep Water was also observed in the Cretan Sea during summer 1987; from that year, the Aegean Sea would have been steadily filled by CDW [*Theocharis et al.*, 1999]; and (6) the occurrence of two successive winters (1991–1992 and 1992–1993) with strong and deep convection in all the Aegean Sea; these convection events are triggered by strong surface heat losses during these winters [*Josey*, 2003].

[6] All these preconditioning factors (or at least some of them) could have changed the Aegean Sea stratification, leading to a less stable water column that was then easily mixed during the very cold 1992 and 1993 winters. They support the hypothesis of the key role played by the cold winters, which corresponds to a quick triggering of the EMT. Another hypothesis is the steady slow filling of the Aegean Sea by dense waters during a long period covering the 1970s and the 1980s, with the winters 1992 and 1993 on top of it, which corresponds to a long-term triggering of the EMT.

[7] Despite the fact that in-situ observations were crucial to discover the EMT and to start proposing hypotheses, they can not give a clear 4D description of the present ocean and do not allow to clearly sort out between the various proposed hypotheses leading to EMT. In addition, they do not allow to answer if other EMT-like events occurred in the past (in the 1970s as proposed by *Josey* [2003]) or could appear in the future under climate change scenarios [*Somot et al.*, 2006]. The full understanding of the sequence of the EMT events and the forecasting of a possible next one can only rely on a high-quality and well-validated numerical modeling of the MTHC during the past decades, as underlined by the recent review made by *Roether et al.* [2007].

[8] The various preconditioning factors mentioned above as well as our knowledge of the complexity and variability of the MTHC allow us to draw the required conditions of a useful modeling exercise of the EMT. High resolutions in space and time are required for the ocean model as well as for the air-sea fluxes used to force it. Long-term simulations covering at least the 1970s, 1980s, and 1990s are needed in order to determine the causing effects. These simulations have to be continued after the 1990s (M. Herrmann et al., What induced the exceptional 2005 convection event in the northwestern Mediterranean basin? Answers from a modeling study, submitted to *Journal of Geophysical Research*, 2010) to quantify the impact of the EMT on the western Mediterranean during the last decade, as observed by *Schroeder et al.* [2008]. The salinity forcing and its interannual variations should be taken into account in order to assess the possible salinity preconditioning issue by the 1980s reduced net precipitation and/or by the changes in the Black Sea freshwater inputs. Consequently, surface salinity relaxation towards climatology should be avoided, as well as any other modeling trick limiting the spatial and temporal variability of the 3D thermohaline structure. Both the eastern Mediterranean and the western Mediterranean should be taken into account and a good representation of the Cretan straits is required. A stable state of the MTHC and water mass characteristics should be reached before the EMT period.

[9] Compared to the numerous papers dealing with the EMT and possible explanations, there are only few papers on modeling studies and even less using long-term realistic atmospheric forcing. Modeling studies which have tried to deal with EMT causes are mainly process studies and their results are inadequate to be directly and quantitatively compared with actual observations. Early studies were done with relatively low resolution ocean models, at sub-basin or basin scales; these studies used atmospheric fields at low spatial and temporal resolutions (monthly data at about $1° \times 1°$, such as COADS or ERA15 data sets) to force the ocean models [*Samuel et al.*, 1999]. These studies were often carried out on short periods of time [e.g., *Rupolo et al.*, 2003]. However, they could give interesting preliminary insights into the EMT. In particular, *Samuel et al.* [1999] found that between 1980–1987 and 1988–1993, the wind driven circulation was modified and thus the locations of the deep water production too. This may have played a role in the EMT. Nevertheless, they did not take into account the important observed changes in air-sea fluxes.

[10] To reproduce the convection in the Aegean Sea, ad-hoc modifications of the air-sea forcing or artificial flux anomalies were sometimes used, for example by *Wu et al.* [2000], who increased freshwater loss over the eastern Mediterranean or decreased sea surface temperature of the Aegean Sea by 1–2°C for chosen winters. By increasing the temporal resolution of the atmospheric fields, *Lascaratos et al.* [1999] and then *Nittis et al.* [2003] were able to reproduce strong convection events, although they modified artificially the freshwater forcing for some chosen years (−40% and −25% for precipitation and Black Sea inputs respectively in 1989, 1990, 1992, and 1993). By increasing the spatial resolution of the atmospheric fields, *Bozec et al.* [2006] argued that an EMT-like event can be partly reproduced using random forcing and highlighted the need for using atmospheric fields with relatively high spatial resolution (about 50 km) to simulate an EMT-like event. But in all of these studies, no realistic interannual freshwater forcing was applied

because of the use of Sea Surface Salinity relaxation toward a climatology.

[11] The goals of this study are the following: (1) to assess how good is a state-of-the-art hindcast simulation in reproducing the sequence of the EMT events; (2) to sort out some of the preconditioning hypotheses proposed in the literature by using a numerical approach: in detail, we would like to assess the role of the interannual variability of the freshwater forcings in controlling the EMT preconditioning and convective phase (none of the previous numerical studies was able to solve the issue of a realistic interannual freshwater forcing); (3) to complete the sequence of the EMT events for the periods not covered by in-situ observations (namely in 1993 for the dense CDW outflow); (4) to better quantify the EMT event in terms of rate of formation, spreading paths and processes using the high-resolution 4D view offered by an ocean model; and (5) to highlight the weak points of the present hindcast design and to propose ways of improvement for future runs.

[12] To reach our objectives, we use an eddy-permitting Mediterranean Sea model NEMOMED8 [*Sevault et al.*, 2009], based on the NEMO engine [*Madec*, 2008]. In this work, NEMOMED8 is forced by a 50-km resolution dynamical downscaling of the ERA40 reanalysis, the so-called ARPERA data set [*Herrmann and Somot*, 2008; *Tsimplis et al.*, 2008] over the 1961–2000 period. Then, three hindcast simulations are done using climatological or realistic interannual freshwater forcing (Atlantic waters, river runoff, Black Sea inflow).

[13] In section 2, we describe the ocean model, its forcing and the simulations. In section 3, we proposed an overall validation of the reference run. Results concerning the EMT, based on the reference run and sensitivity simulations, are detailed in section 4. Conclusion and perspectives are discussed in section 5.

2. Model and Simulations

2.1. Model Grid and Bathymetry

[14] The NEMOMED8 model [*Beuvier et al.*, 2008; *Sevault et al.*, 2009] is a Mediterranean configuration of the NEMO ocean model [*Madec*, 2008], following the previous works done with OPAMED8 [*Somot et al.*, 2006; *Somot and Colin*, 2008; *Herrmann et al.*, 2008; *Tsimplis et al.*, 2008, 2009], which is a regional configuration of the OPA ocean model [*Madec et al.*, 1998].

[15] NEMOMED8 covers the whole Mediterranean Sea plus a buffer zone including a part of the near Atlantic Ocean. It does not cover the Black Sea. The horizontal resolution of NEMOMED8 is $1/8° * 1/8° \cos(\phi)$, with ϕ the latitude. This is equivalent to a range of 9 to 12 km from the north to the south of the Mediterranean domain, with square meshes. The NEMOMED8 grid is tilted and stretched at the Gibraltar Strait in order to better follow the SW-NE axis of the real strait and to increase the local resolution up to 6 km [*Béranger et al.*, 2005; *Drillet et al.*, 2005]; the Gibraltar Strait is represented with a two-grid-point wide strait. A time step of 20 minutes is applied.

[16] NEMOMED8 has 43 vertical Z-levels with an inhomogeneous distribution (from $\Delta Z = 6$ m at the surface to $\Delta Z = 200$ m at the bottom with 25 levels in the first 1000 m). The bathymetry is based on the ETOPO $5' \times 5'$ database [*Smith and Sandwell*, 1997]. We use a partial cell parametrization, i.e., the local deepest level in the model has a variable depth in order to fit the real bathymetry (Figure 1).

[17] The evolution of the surface of the sea is parameterized by a filtered free-surface [*Roullet and Madec*, 2000]. With this parametrization, the volume of the Mediterranean Sea is not conserved, given the loss of water induced by the surface evaporation. In order to conserve the volume, at each time step, the evaporated water over the whole basin is redistributed in the Atlantic buffer zone west of 7.5°W.

2.2. Physics

[18] The horizontal eddy diffusivity is fixed to 125 $m^2.s^{-1}$ for the tracers (temperature, salinity) using a Laplacian operator (the diffusion is applied along iso-neutral surfaces for the tracers) and the horizontal viscosity coefficient is fixed to -1.0×10^{10} $m^4.s^{-2}$ for the dynamics (velocity) with the use of a biharmonic operator. A 1.5 turbulent closure scheme is used for the vertical eddy diffusivity [*Blanke and Delecluse*, 1993] with an enhancement of the vertical diffusivity coefficient up to 50 $m^2.s^{-1}$ in case of unstable stratification. A no-slip lateral boundary condition is used and the bottom friction is quadratic. The TVD scheme [*Barnier et al.*, 2006] is used for the tracer advection. The solar radiation can penetrate into the ocean surface layers [*Bozec et al.*, 2008].

2.3. Forcing

2.3.1. Atmospheric Forcing

[19] The atmospheric forcing comes from a dynamical downscaling of the ERA40 reanalysis from the ECMWF [*Simmons and Gibson*, 2000] (resolution of 125 km) by the regional climate model ARPEGE-Climate developed at CNRM [*Déqué and Piedelievre*, 1995] (grid stretched over the Mediterranean Sea, resolution of 50 km). The dynamical downscaling, named ARPERA [*Herrmann and Somot*, 2008; *Somot and Colin*, 2008; *Tsimplis et al.*, 2008], includes a spectral nudging [*Von Storch et al.*, 2000]. A relaxation is applied to the spectral coefficients corresponding to the first 63 wave numbers for the following prognostic variables: temperature, vorticity, divergence, logarithm of the surface pressure (not for the humidity). Thus, the small scales of ARPEGE-Climate (scales under 250 km) are let free and the larger scales are driven by ERA40. This dynamical downscaling technique allows us to obtain forcings with high resolution and a real temporal chronology and constitutes somehow a "poor-man" regional reanalysis (see also *Sotillo et al.* [2005] for another "poor-man" regional reanalysis technique).

[20] In this study, NEMOMED8 is forced by ARPERA daily mean fields of momentum, freshwater flux (Evaporation minus Precipitations) and net heat flux. The latter is applied with a relaxation term using the ERA40 Sea Surface Temperature (SST). This term plays actually the role of a first order coupling between the SST of the ocean model and the atmospheric heat flux [*Barnier et al.*, 1995]. This term ensures a consistency between the surface heat fluxes coming from the atmosphere and the SST calculated by the ocean. The value of the relaxation coefficient is -40 $W.m^{-2}.K^{-1}$, as with *CLIPPER Project Team* [1999], without spatial variation. It is equivalent to an 8-day restoring time scale for a layer of 6m [*Somot et al.*, 2006].

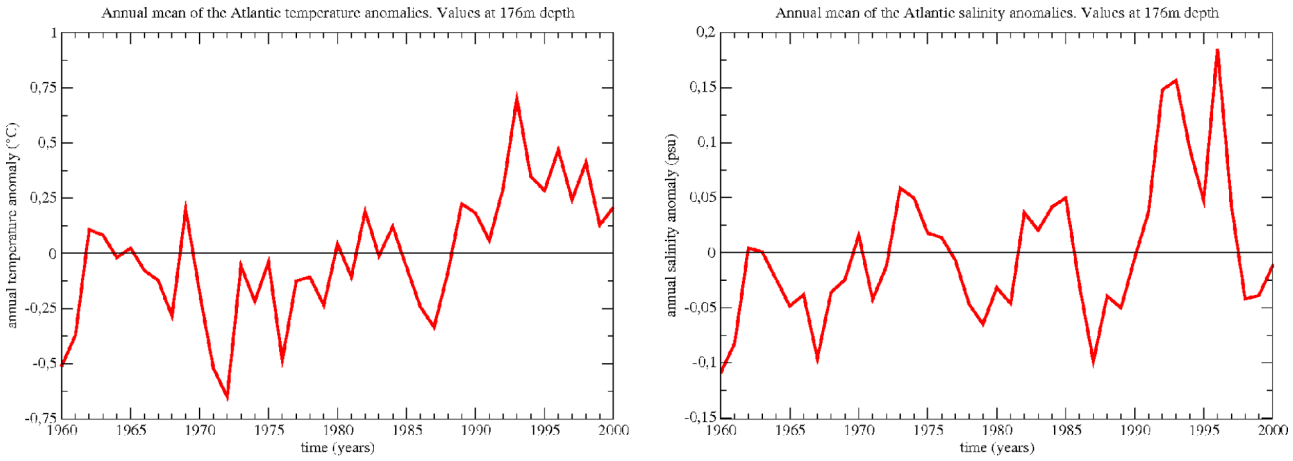

Figure 2. Annual mean of the anomalies of (left) temperature (in °C) and (right) salinity (in psu) introduced in the Atlantic buffer zone (based on *Daget et al.* [2009]). Values at 176 m depth. These anomalies are added to the seasonal climatology of *Reynaud et al.* [1998]; at this depth, the annual temperature and salinity averaged over the Atlantic buffer zone in this climatology are respectively 14.37°C and 36.05 psu.

2.3.2. Atlantic Forcing

[21] The exchanges with the Atlantic ocean are performed through a buffer zone. From 11°W to 7.5°W, 3D temperature and salinity of the model are relaxed towards T-S climatological fields. This relaxation is a Newtonian damping term in the tracer equation, equal to $-(X_{model} - X_{climatology})/\tau$. The restoring term is weak west of Cadiz and Gibraltar area (τ = 100 days at 7.5°W) and stronger moving westwards from it (τ = 3 days at 11°W). In the Atlantic zone, two different climatologies were used: the seasonal climatology of *Reynaud et al.* [1998] which is perpetual in year, and the interannual monthly data set of *Daget et al.* [2009], based on a long-term ocean reanalysis that covers the twentieth century. Figure 2 shows the yearly-averaged anomalies of temperature and salinity of this new interannual data set at 176 meters depth in the Atlantic zone with respect to the Reynaud climatology; these are the typical anomalies which will cross the Gibraltar Strait towards the Mediterranean Sea.

2.3.3. Explicit River Runoff Fluxes

[22] The river inputs are explicitly added as a freshwater flux to complete the surface water budget. Two different data sets, giving the monthly runoff of 33 Mediterranean rivers listed in the RivDis database, were used: a climatology computed from the RivDis database [*Vörösmarty et al.*, 1996] and another data set with interannual variations of the annual runoff based on the work of *Ludwig et al.* [2009] (but with a single seasonal cycle for each river). The annual values of the runoff of major rivers for these two data sets are plotted in Figure 3, highlighting the high variations of the Nile, the Rhone and the Po rivers during the end of the twentieth century.

2.3.4. Black Sea Inputs

[23] The Black Sea is not included in NEMOMED8. Nevertheless, this sea can be considered as one of the major freshwater sources for the Mediterranean Sea. The exchanges between the Black Sea and the Aegean Sea consist of a schematic two-layer flow across the Sea of Marmara and the Dardanelles Strait [*Oguz and Sur*, 1989]. In this study, we assume that this two-layer flow can be approximated by a freshwater flux diluting the salinity at the ocean grid point, corresponding to the net Black Sea discharge through the Dardanelles Strait. Then, the Black Sea input is modeled as a river runoff in the Aegean Sea. The heat exchanges between the Aegean Sea and the Black Sea are not taken into account. The monthly mean equivalent water flux towards the Aegean Sea is computed as the net water budget over the Black Sea surface: Precipitation + Black Sea Rivers Runoff-Evaporation, with the hypothesis that the Black Sea level does not change over a long period of time. In this study we use two different data sets, as shown in Figure 3: the climatology of *Stanev et al.* [2000] and an interannual derived data set using the same method and the same monthly cycle [*Stanev and Peneva*, 2002]. Figure 3 underlines that the variations of the river forcing are dominated by the variations of the Black Sea inflow. It also shows the importance of the interannual variations of the Black Sea inflow, which will play a significant role in the freshwater budget of the Aegean Sea.

2.3.5. Balancing the Water Budget

[24] In order to avoid any surface salinity damping in NEMOMED8, in contrast with previous studies, a correction of the E-P-R flux at a monthly frequency is applied [*Somot*, 2005]. These monthly corrections have been computed by averaging the Sea Surface Salinity (SSS) relaxation term through a separate simulation (Figure 4). The relaxation is necessary to compensate inaccuracy in the freshwater forcings from the atmospheric models. The surface freshwater budget is thus balanced without altering the spatial and temporal variations of the freshwater flux and so of the SSS. In annual mean, the correction has value of 0.20 m.yr^{-1}, increasing the net surface evaporation by about 10% (Figure 4). This correction term is added to the water fluxes coming from the atmospheric fields and from the river runoff.

2.4. Initial Condition, Spin-Up, and Simulations

[25] First, we carried out a fifteen-year spin-up. The initial state is given by the MEDATLAS-II climatology for the

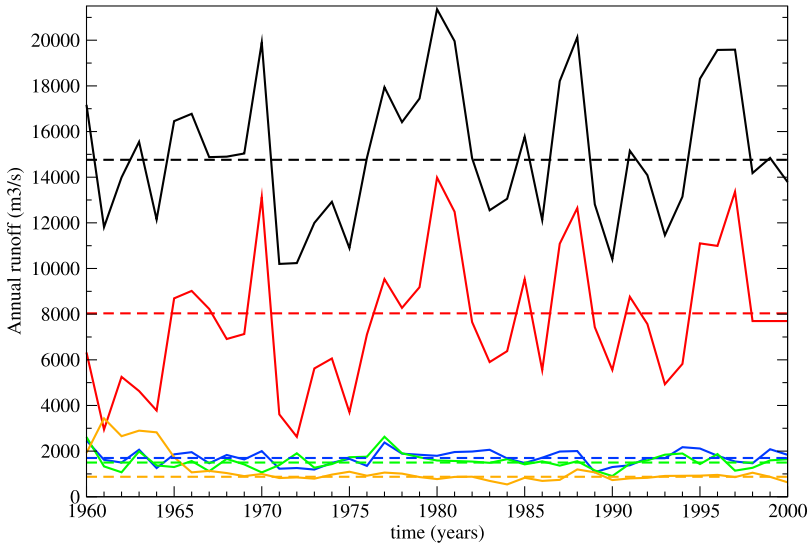

Figure 3. Annual runoff (in $m^3.s^{-1}$) for the Black Sea (in red), the Nile river (in orange), the Rhone river (in blue), the Po river (in green) and the sum of all river runoffs and the Black Sea inflow used in this study (in black). The solid lines are the values for NM8-atl-riv and NM8-riv (based on *Ludwig et al.* [2009] and *Stanev and Peneva* [2002]), and the dashed lines are the climatological values for NM8-clim (based on *Vörösmarty et al.* [1996] and *Stanev et al.* [2000]).

Mediterranean part of the model [*MEDAR-MEDATLAS Group*, 2002], and by the *Reynaud et al.* [1998] climatology for the Atlantic buffer zone. During five years, the model ran with 3D dampings towards the initial climatologies for temperature and salinity with a restoring time-scale of 10 days, forced by the ARPERA fluxes from 1960 to 1965, with climatological hydrological forcings (river runoff, Black Sea inflow and Atlantic buffer zone). Then, the model ran in a free mode during 10 years, forced by the ARPERA fluxes from 1960 to 1970, and still with climatological hydrological forcings.

[26] Starting at the end of the spin-up, three companion simulations are carried out from August 1960 to December 2000 (Table 1). The first one, hereinafter NM8-atl-riv, uses the interannual data sets for the river runoff, the Black Sea inflow and the Atlantic water characteristics in the buffer zone; it will be the reference simulation. The second one, hereinafter NM8-riv, has climatological Atlantic waters and

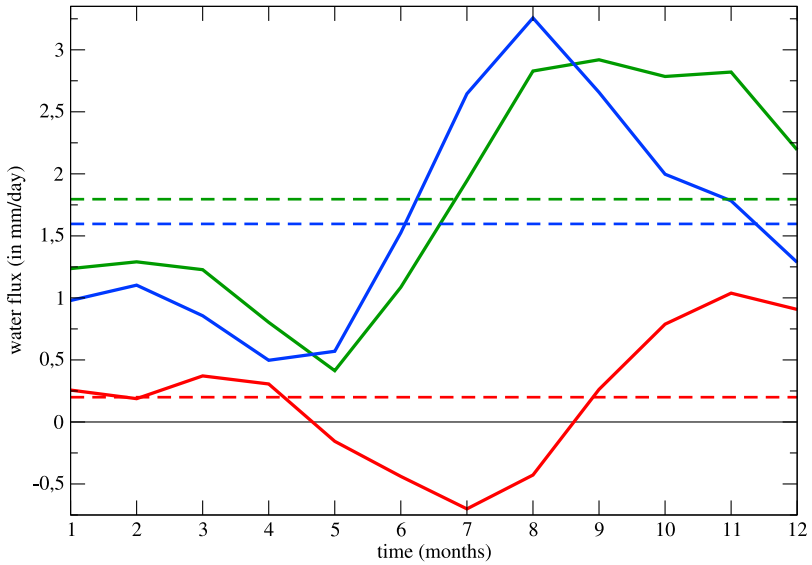

Figure 4. Values of the monthly cycle (solid lines) and of the annual mean (dashed lines) of different components of the surface freshwater flux (in $mm.day^{-1}$): E-P-R without correction (blue), additive correction (red), and E-P-R + correction (green). In winter the correction adds evaporation, and in summer it adds precipitation.

Table 1. Differences in the Hydrological Forcings Between the Three Companion Simulations

	Climatological River Runoff [*Vörösmarty et al.*, 1996] and Black Sea Input [*Stanev et al.*, 2000]	Interannual River Runoff [*Ludwig et al.*, 2009] and Black Sea Input [*Stanev and Peneva*, 2002]	Climatological Atlantic Buffer Zone [*Reynaud et al.*, 1998]	Interannual Atlantic Buffer Zone [*Daget et al.*, 2009]
NM8-atl-riv		Yes		Yes
NM8-riv		Yes	Yes	
NM8-clim	Yes		Yes	

still interannual river runoff and Black Sea input. The third one, hereinafter NM8-clim, has climatological forcing for the river runoff and Black Sea inflow as for the Atlantic area.

3. General Features

3.1. Basin-Scale Circulation

[27] In this section, we describe the general features of the reference simulation NM8-atl-riv. The results obtained with the two other sensitivity experiments are generally close to this one.

[28] The general dynamic features of the Mediterranean Sea are illustrated in Figure 5 by the 40-year mean Sea Surface Height (SSH) and currents at 35 m depth. The general cyclonic path of AW is well reproduced. In particular, three intense cyclonic gyres, where winter convection generally occurs, are noticed in the Gulf of Lion, in the southern Adriatic Sea and in the Levantine basin (Rhodes gyre). The anticyclonic gyres in the Alboran Sea are also well simulated (especially the most eastern one), as the coastal current along the African coasts, with meanders along its path, and the Asia Minor Current (AMC) along the Turkish coasts.

[29] Linked to this general circulation, the water budget of the simulations (Table 2) is practically perfectly balanced: the net water transport at the Gibraltar Strait balances the water loss at the Mediterranean surface (budget closed at less than 0.01 m.yr^{-1}). The inflow at the Strait of Gibraltar is +0.87 Sv, the outflow is −0.82 Sv, given a net flow of +0.05 Sv (1 Sv = 10^6 m^3.s^{-1}). These values are in good agreement with the observations, which give values ranging between +0.72 and +1.01 Sv for the inflow, between −0.68 and −0.97 Sv for the outflow and between +0.04 and +0.10 Sv for the net flow (see Table 3).

3.2. Salt and Heat Budgets

[30] The salt budget (Table 2) is also well balanced: the net salt transport at the Gibraltar Strait is responsible for the salt content trend of the whole Mediterranean Sea (budget closed at less than 10^{-4} psu.y^{-1}). There is no salt flux at the sea surface.

[31] The heat budget is nearly equilibrated as well (budget closed at 0.4 W.m^{-2}). In this budget, four components have to be taken into account: the heat transport at the Gibraltar Strait and the Mediterranean heat content trend as before, but also two added heat exchanges at the sea surface. Indeed, on top on the net heat flux coming from the atmospheric forcing, the gains or losses of water mass induce gains or losses of heat. This latter term is due to the free surface scheme. To compute it, we assume that the temperature associated to this water mass flux is the modeled Sea Surface Temperature. It is the case for the water which evaporates but it is an approximation for the precipitation (temperature of the raindrops) and the runoff (temperature of the rivers). As we use monthly values to compute the heat exchange due to water mass variations at the sea surface, which is proportional to $(R + P - E) * SST$ (with R the river

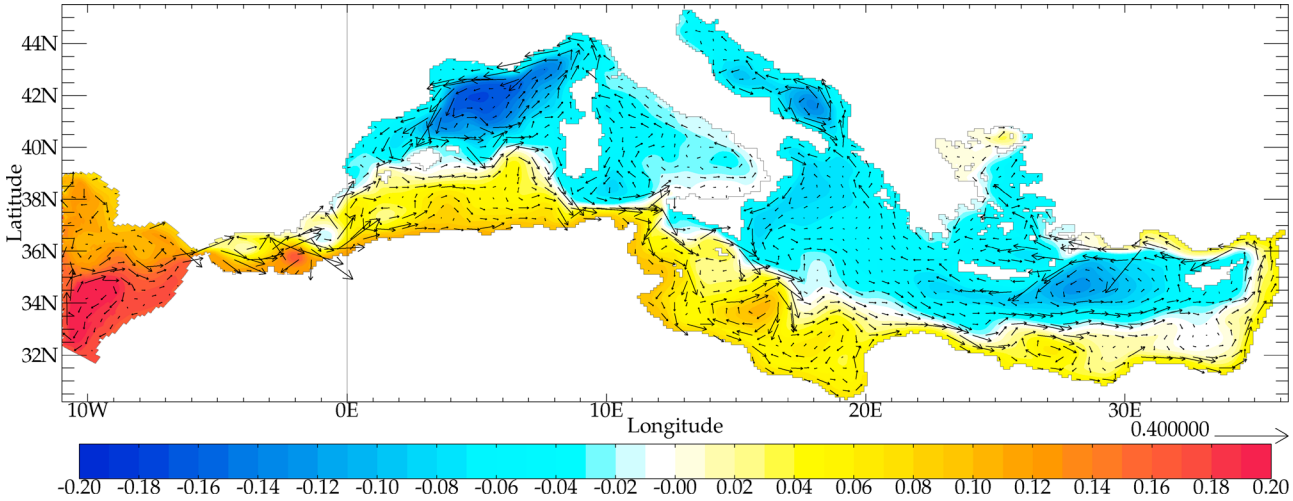

Figure 5. Sea surface height (colored field, in m) and currents at 35m depth (vectors, in m.s^{-1}), averaged on 1961–2000 for NM8-atl-riv. One vector in four is plotted.

Table 2. Water, Heat, and Salt Budgets for the Whole Mediterranean Over the 40 Years of the Simulation NM8-atl-riv[a]

Budget Components	Mean and Standard Deviation Over 1961–2000
Water inflow at Gibraltar	0.87 ± 0.03 Sv
Water outflow at Gibraltar	−0.82 ± 0.03 Sv
Net water transport at Gibraltar	0.05 ± 0.01 Sv, i.e., 0.65 ± 0.07 m.yr^{-1}
Water flux trough the surface	0.65 ± 0.07 m.yr^{-1}
Heat flux from the surface	−5.2 ± 4.9 W.m^{-2}
Heat transport at Gibraltar	+5.2 ± 0.5 W.m^{-2}
Mediterranean heat content trend	+0.002°C.yr^{-1}, i.e., +0.4 W.m^{-2}
Salt transport at Gibraltar	+0.0009 psu.yr^{-1}
Mediterranean salt content trend	+0.0009 psu.yr^{-1}

[a]The values are globally the same for NM8-riv and NM8-clim.

runoff, *P* the precipitation, *E* the evaporation and *SST* the sea surface temperature), we suggest that the missing 0.4 W.m^{-2} in the heat budget may be attributed to the daily time-scale. Nevertheless, the total surface heat flux, −5.2 ± 4.9 W.m^{-2} (Table 2), has a good interannual variability and is in very good agreement with the −5.2 ± 1.3 W.m^{-2} estimate of *Macdonald et al.* [1994]. It is worth noting that in this total surface heat flux, the 40-year mean of the relaxation term amounts +11.5 W.m^{-2}. This term plays the role of a first order coupling between the SST of the ocean model and the atmospheric heat flux. It also acts as a correction which accounts for the feedback of the ocean on the air-sea fluxes and in a lesser extent compensates for uncertainties in air-sea fluxes estimates. It is important to focus on the problem of closing these heat and salt budgets since we carried out long term simulations dedicated to the study of trends or decadal events.

3.3. Variations of Heat and Salt Contents in the Mediterranean Sea

[32] In this part, we do a comparison (Figure 6), for the 40-year studied period, between the annual averaged heat and salt contents in the three simulations and the interannual gridded database of *Rixen et al.* [2005]. Following this article, the values are presented in mean for the whole water column and over three vertical layers, representative of the major water masses in the Mediterranean Sea. These three layers are: the 0–150 m surface layer corresponding to the AW, the 150–600 m intermediate layer mainly filled by the LIW and the deep layer below 600 m where the WMDW and EMDW are found. The anomalies presented in Figure 6 are computed for the model outputs and the interannual database with respect to their own 1961–2000 mean (see Table 4).

[33] The basin-wide heat content (Figure 6a) is almost the same for the three simulations over the 40 years. It could be expected since the three runs differ in the freshwater forcing, which then affect especially the salt content and in a lesser extent the heat content. Thus, only slight differences between the heat contents in the three simulations are noticed in the 1970s. For the three experiments, a mean bias of +0.1°*C* is noticed if compared to *Rixen et al.* [2005] (Table 4), but the interannual variations are well represented. In fact, the correlation coefficient between the simulations and the database for the heat content is larger than 0.73 for the three simulations (Table 4).

[34] The basin-wide salt content (Figure 6b) is also in good agreement with the database. It does not show any noticeable bias if compared to *Rixen et al.* [2005], but its interannual variations are too weak. An encouraging point is that the correlation with the database is becoming significant (at 95% level) with the introduction of interannual hydrological forcings in the two simulations NM8-atl-riv and NM8-riv (the correlation coefficient is 0.33 instead of being non significant for NM8-clim, see Table 4).

[35] By examining furthermore the three layers mentioned above, we do not notice large differences between the experiments. In the surface layer (Figure 6c), an accurate simulation of the values and the interannual variations of the surface heat content is noticed, which is probably due to the chronology in the forcing fields given at large scales by ERA40 and to the relaxation towards the Sea Surface Temperature of ARPERA. But, the salt content of this layer shows differences in the time variations. Its values are quite good before 1970, but then the simulations show a freshening of the surface waters by more than 0.1 psu in 10 years, giving a total 40-year bias of −0.09 psu (Table 4).

[36] In the intermediate layer, due to a slight drift during the spin-up, the heat content is too high of about +0.2°*C* for the three simulations. However, the interannual variability is very well reproduced: the correlation coefficient is greater than 0.66 for the three experiments (Table 4). In the 1970s, the observations show a slight heat content increase in the intermediate layer. But, it has recently been explained that this warming corresponds to a positive artefact in the measurements done with shallow XBT [*Wijffels et al.*, 2008]. Even if the value of the correlation coefficient is high for NM8-clim (0.85), it is biased by the wrong warming in the 1970s. Thus, for the intermediate layer, we can suppose that NM8-atl-riv and NM8-riv have a better general behavior than the one of NM8-clim, despite the uncertainty in the observations. For the salt content at intermediate depth, the simulations are too salty (+0.05 psu) and do not reproduce the interannual variations reported in the observations.

[37] The interannual variations of the heat content are weaker in the bottom layers than in the upper layers. The simulations reproduce this fact, but the model overestimates the observed positive trend of the heat content. Over the 40 years, this leads to a mean bias of + 0.07°*C* (Table 4). The positive trend of the salt content is also well simulated, but its interannual variations are underestimated compared to the observed one, as already noticed for the other layers. However, we suggest that the interannual variations of the salt content for all layers and of the deep heat content could be overestimated in the *Rixen et al.* [2005] database because of undersampling. That could explain the relatively low agree-

Table 3. Estimates of the Water Inflow and Outflow at the Gibraltar Strait[a]

Authors	Inflow	Outflow
Bryden and Kinder [1991]	+0.92	−0.88
Bryden [1994]	+0.72 ± 0.16	−0.68 ± 0.15
Tsimplis and Bryden [2000]	+0.78	−0.68
Candela [2001]	+1.01	−0.97
Baschek et al. [2001]	+0.81 ± 0.07	−0.76 ± 0.07
This study	+0.87 ± 0.03	−0.82 ± 0.03

[a]Estimates are given in Sv.

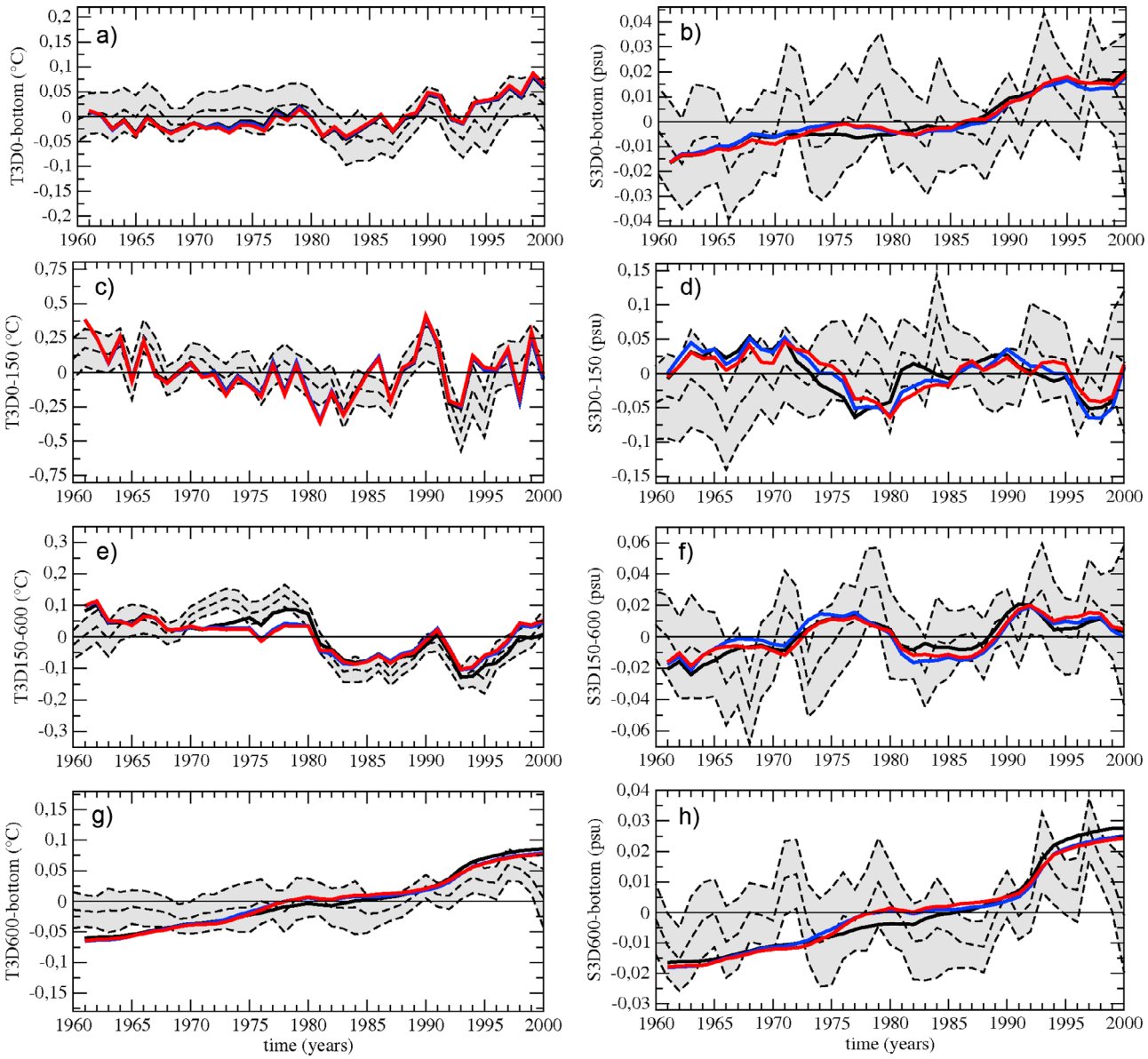

Figure 6. (a, c, e, and g) Heat content anomalies (T3D in °C) and (b, d, f, and h) salt content anomalies (S3D in psu) for different layers of the Mediterranean Sea: the whole water column (0 m–bottom, Figures 6a and 6b), the upper layer (0–150 m, Figures 6c and 6d), the intermediate layer (150–600 m, Figures 6e and 6f), and the deep layer (600 m–bottom, Figures 6g and 6h). The simulations are in solid lines: NM8-atl-riv (red), NM8-riv (blue), and NM8-clim (black). The interannual gridded database of *Rixen et al.* [2005] is show as black dashed lines, with the ±1 standard deviation interval in grey. The scales are chosen so that the salt content scales are five times lower than the heat content scales (same impact on potential density). The anomalies are computed for the simulations and the database with respect to their own 1961–2000 mean.

ment between simulations and observations in those cases, both in terms of bias and correlation.

[38] In conclusion, there is a global agreement between the simulations and the observations, especially for the temperature. The variations of the heat content are well reproduced while those of the salt content less. The main bias is in the intermediate layer, which is slightly too warm and too salty. As there are in general the same trends and variations for the three experiments, we will focus in the following on the simulation with the most realistic hydrological forcings: NM8-atl-riv.

4. EMT

[39] In this section, we focus on the modeling of the EMT in the NM8-atl-riv simulation, with a chronological investigation. We look at the stratification in the Aegean Sea to determine the ocean state and the circulation changes in the

Table 4. Characteristics of the Three Simulations Over 1961–2000: Heat and Salt Content for Different Layers of the Whole Mediterranean Sea[a]

	Mean Over 1961–2000				Mean Bias			Correlation		
	atl-riv	riv	clim	Rixen	atl-riv	riv	clim	atl-riv	riv	clim
Heat content (in °C)										
Total	13.79	13.79	13.79	13.69	+0.10	+0.10	+0.10	0.73	0.76	0.78
0–150 m	16.26	16.26	16.26	16.30	n.s.	n.s.	n.s.	0.69	0.68	0.68
150–600 m	14.27	14.27	14.28	14.07	+0.20	+0.20	+0.21	0.66	0.69	0.85
600 m–bottom	13.32	13.32	13.32	13.25	+0.07	+0.07	+0.07	0.54	0.54	0.68
Salt content (in psu)										
Total	38.62	38.62	38.62	38.62	n.s.	n.s.	n.s.	0.33	0.33	n.s.
0–150 m	38.27	38.27	38.27	38.36	−0.09	−0.09	−0.09	n.s.	n.s.	n.s.
150–600 m	38.76	38.76	38.76	38.71	+0.05	+0.05	+0.05	n.s.	n.s.	n.s.
600 m–bottom	38.63	38.63	38.63	38.62	n.s.	n.s.	n.s.	0.43	0.48	0.50

[a]Here n.s. means "non-significant," the value is inside the ±1 standard deviation of the interannual gridded database of *Rixen et al.* [2005]. The given correlations are computed after removing trends, for both the simulations NM8- and the database of *Rixen et al.* [2005]. Significant correlations are those with values outside the 95% confidence interval (significantly different from zero if the absolute value of the correlation is larger or equal than 0.31).

eastern Mediterranean before the EMT period. Then, the intensity of the surface fluxes, which force the Aegean Sea and cause the winter convection, is assessed. After the filling of the Aegean Sea with dense waters, we look at their overflow and their spreading in the eastern Mediterranean. Then, we compare the sensitivity simulations NM8-clim and NM8-riv to the reference one in order to quantify the impacts of the changes in the hydrological forcing on the sequence of the EMT events.

4.1. Preconditioning of the Aegean Convection

[40] Let us consider the EMT preconditioning period as the years and months before the beginning of winter 1991–1992, so the period before November 1991. Indeed, the EMT can be considered starting in the Aegean Sea by the severe surface heat and water losses during winter 1991–1992, followed then by another severe winter in 1992–1993.

4.1.1. Changes in the Levantine Surface Circulation

[41] As mentioned in section 1, some of the hypotheses about the preconditioning of the EMT concern changes in the surface circulation (modified path of the AW, three anticyclonic eddies south of Crete modifying the LIW path), both having as a consequence an increase of the salinity of the Aegean Sea during the late 1980s and early 1990s. Here, we are going to examine if these circulation changes are reproduced in the model, in order to answer whether it is an important triggering element of the EMT in the simulation.

[42] We look at the upper and intermediate circulations, at about 100 and 300 m depth in average over 1988–1991, in order to focus on the period just prior to the EMT and to compare the model results to the observations made by *Malanotte-Rizzoli et al.* [1999] in 1991. The salinity and the currents for 1961–1987 and for 1988–1991 at these depths are presented in Figure 7, as well as the anomalies with respect to the period 1961–1987. Notice that the vectors on Figures 7e and 7f are anomalies of currents. Figure 7a for 1961–1987 shows the mean simulated sub-surface circulation in the Levantine basin: a cyclonic AW path, the signature of an anticyclonic circulation in the Mersa-Matruh area between 26°E and 28°E, the Asia Minor Current and the Rhodes gyre. These features are still present at 300 m depth (Figure 7b).

[43] Let us focus first on the upper circulation (Figures 7a, 7c, and 7e). In comparison to the 1961–1987 period, we first notice that in 1988–1991 the AW path is modified. While the AW flows close to the Lybian and Egyptian coasts in average during the 1961–1987 period, in 1988–1991 the AW is located offshore at about 100 km north of the Egyptian coasts, between 33°N and 34°N, as shown by the fresh anomaly in Figure 7e. In consequence, the positive salinity anomaly more south, along the Lybian and Egyptian coasts and then off the Near-East and Turkish coasts, shows that less or no AW reaches these areas in the period 1988–1991. Then, a weaker and/or saltier Asia Minor Current leads to a positive salinity anomaly in the Aegean Sea. Thus, in this simulation, a modification of the AW path leads to an increase of the salinity of the surface layer in the far eastern Levantine and in the Aegean Sea.

[44] In the LIW layer (Figure 7b, 7d, and 7f), the anticyclonic eddy signature obvious in the upper circulation is still present at this depth, but the eddies are not at the observed locations which are reported by *Malanotte-Rizzoli et al.* [1999]. However, the current north of the Rhodes gyre is less intense and thus it slows down the LIW transport towards the Ionian basin. Those anticyclonic eddies do not play a key role in modifying the eastward LIW spreading but rather in shifting northward the AW path, preventing its penetration into the far eastern Levantine and the Aegean Sea that would result in a salinity decrease in the surface layers of these regions.

[45] This steady salt increase of the Aegean Sea before 1993 is obvious when one focuses on the variations of the Aegean salt contents (Figures 8b, 8d, 8f, and 8h, red lines for NM8-atl-riv). We mention that the behavior of the sea surface salinity (not shown) is similar with the one of the surface layer salt content. All layers show a salt content increase between 1988 and 1993, with a shift in time from surface to bottom for the maximum salinity. This time-lag indicates that the positive salt anomaly introduced in the surface layer by the circulation changes (and by the dry air-sea fluxes, see section 4.2) propagates to the deep layers due to the vertical mixing during winter convection.

4.1.2. Changes in the Surface Water Fluxes

[46] We determine here whether a period with reduced net precipitation occurred over the eastern Mediterranean during

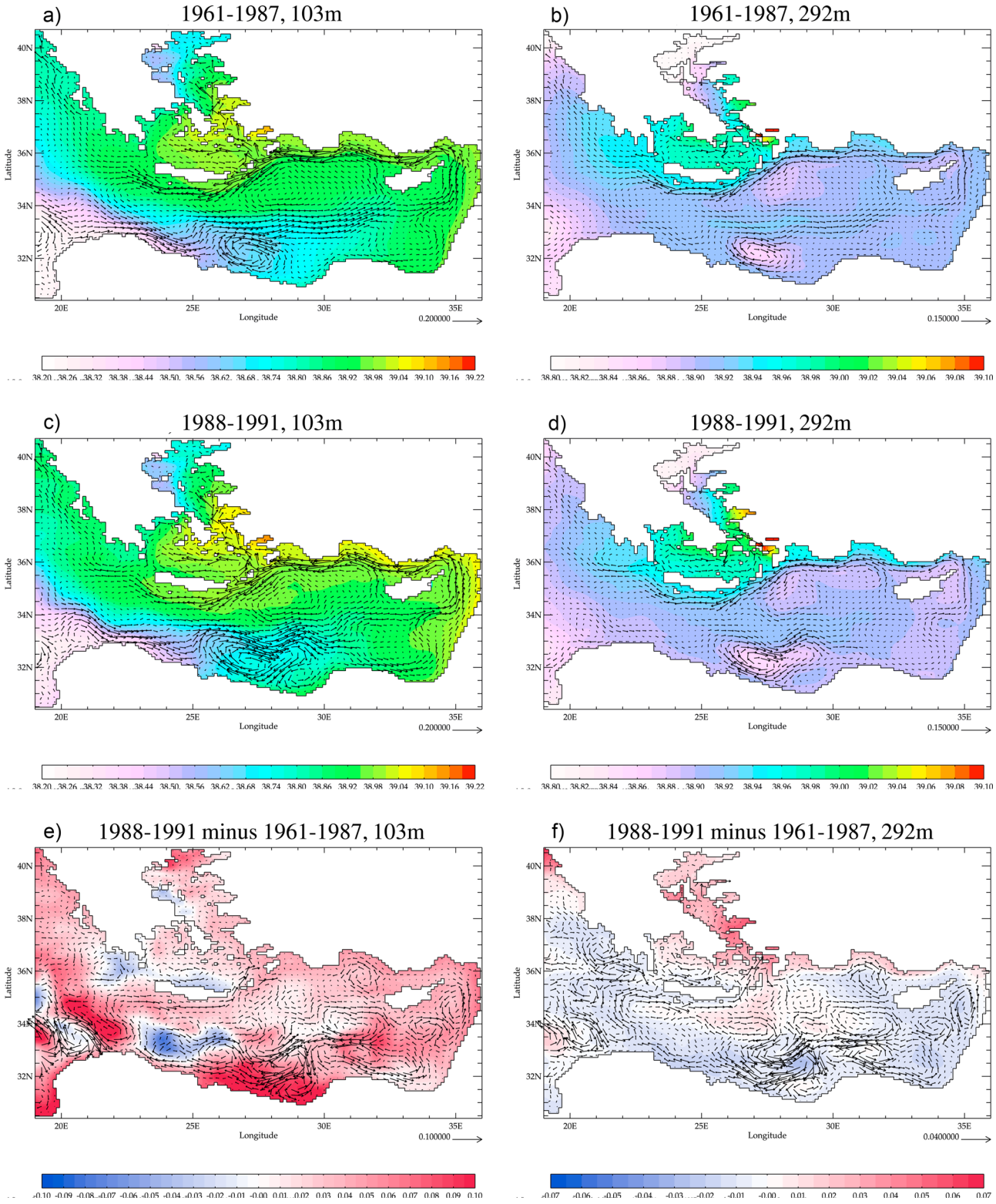

Figure 7. Salinity (colored field, in psu) and currents (vectors, in m.s^{-1}) at (a, c, and e) 103 m and (b, d, and f) 292 m depth in the far eastern Mediterranean, for NM8-atl-riv: 28-year mean over 1961–1987 (figures 7a and 7b), 4-year mean over 1988–1991 (Figures 7c and 7d), and salinity and currents anomalies for the period 1988–1991 with respect to the period 1961–1987 (Figures 7e and 7f). One vector in two is plotted. Scales differ between the 103 m and the 292 m depth plots.

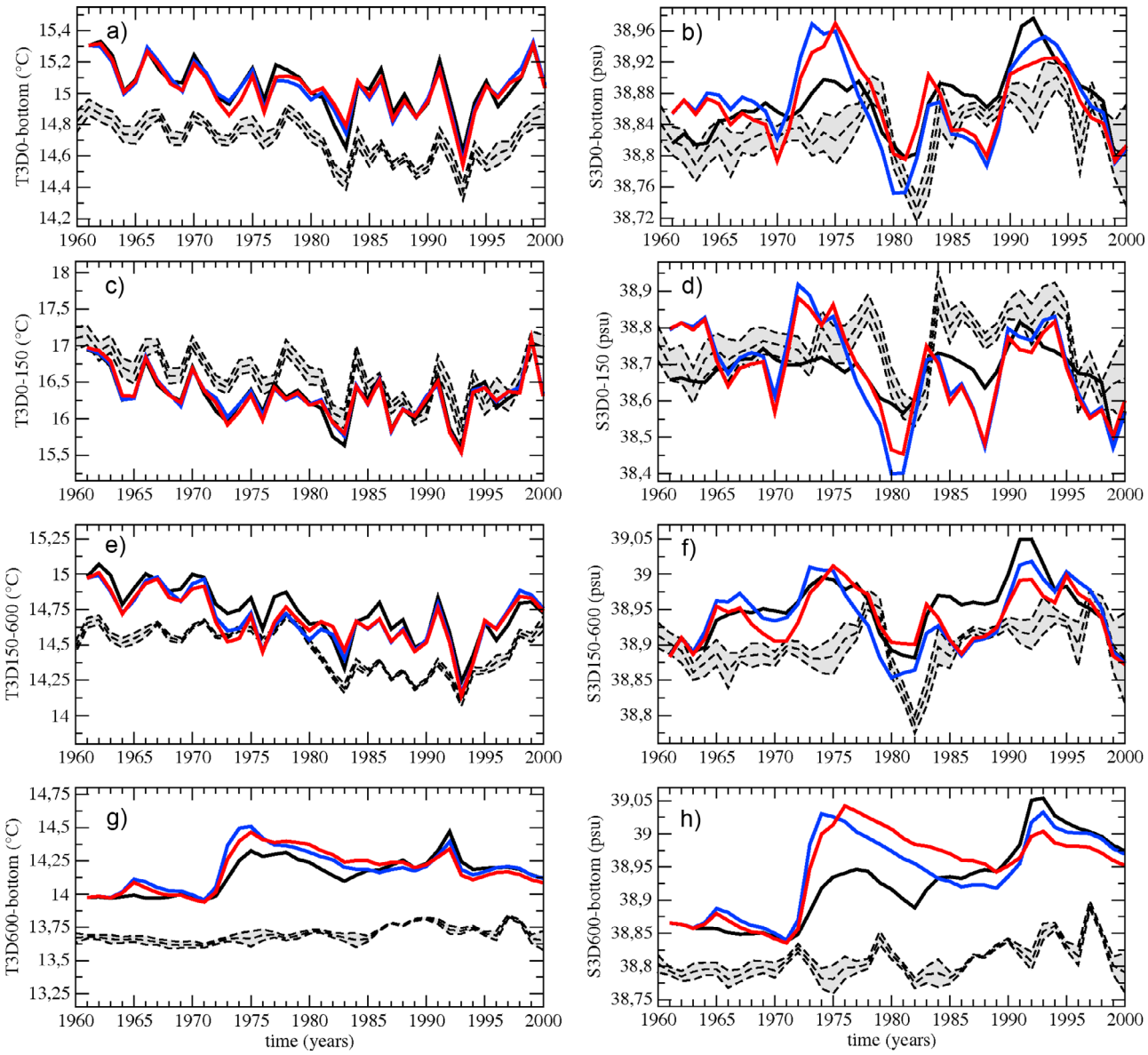

Figure 8. (a, c, e, and g) Heat (T3D in °C) and (b, d, f, and h) salt (S3D in psu) contents for different layers of the Aegean Sea: the whole water column (0 m–bottom, Figures 8a and 8b), the upper layer (0–150 m, Figures 8c and 8d), the intermediate layer (150–600 m, Figures 8e and 8f), and the deep layer (600 m–bottom, Figures 8g and 8h). The simulations are in solid lines: NM8-atl-riv (red), NM8-riv (blue), and NM8-clim (black). The interannual gridded database of *Rixen et al.* [2005] is shown as black dashed lines, with the ±1 standard deviation interval in grey. The scales are chosen so that the salt content scales are five times lower than the heat content scales (same impact on potential density).

the end of the 1980s and to what extent it contributes to the salinity increase of the eastern Mediterranean. Figure 9a displays the annual anomalies of the net surface precipitation flux over the Levantine basin (east of 25°E in the Cretan Passage and south-east of the eastern straits of the Cretan Arc). The 1980s are obviously a period with a reduced freshwater input through the surface, the anomaly of the atmospheric P−E flux amounts −3 cm.yr^{-1} in average over the 11-year 1980–1990 period and with respect to the 1961–2000 period. By taking into account the interannual variations of the runoff, i.e., by considering the anomalies of the total freshwater flux at the surface of the Levantine basin (Figure 9b), the anomaly of the P+R−E flux amounts −5 cm.yr^{-1} in average over 1980–1990. This leads to an increase of the salinity in the surface layer of the far eastern Mediterranean during this 11-year period mentioned before, as it is clearly visible on Figure 7c and 7e.

[47] We here apply the same reasoning as *Josey* [2003] to find the contribution of changes in the net surface evaporation to the salinity increase in the eastern Mediterranean. *Roether et al.* [1996] found that for the observed increase to be explained entirely through surface forcing, the net

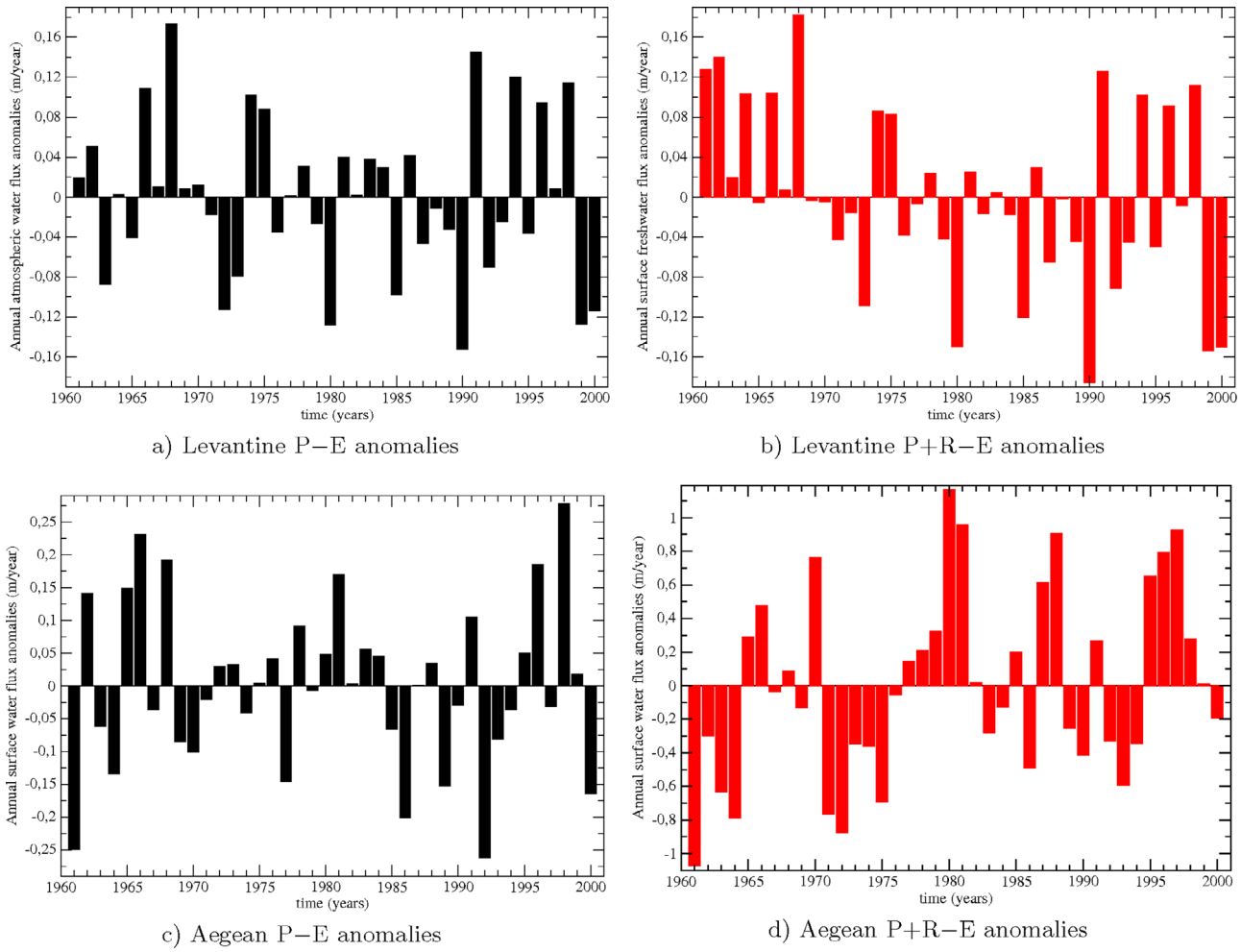

Figure 9. Annual anomalies (in m.yr^{-1}) for (a) the net surface precipitation (P−E) of ARPERA over the Levantine basin, (b) the net surface freshwater flux (P + R−E) over the Levantine basin, (c) the net surface precipitation (P−E) of ARPERA over the Aegean Sea, and (d) the net surface freshwater flux (P + R−E) over the Aegean Sea.

evaporation over the entire eastern Mediterranean must have increased by at least 0.2 m.yr^{-1} over the 7-year period 1988–1994. *Tsimplis and Josey* [2001] have obtained an estimate of the required change in E-P of 0.1 m.yr^{-1}. *Josey* [2003] compared, for the SOC and the NCEP/NCAR atmospheric data sets, the mean values of the net evaporation for the periods 1980–1987 and 1988–1994. He estimated the increase in net evaporation between these two periods to lie in the range 0.02–0.04 m.yr^{-1}, which thus contributes between 10 and 40% of the required change of 0.1–0.2 m.yr^{-1}. In the data from ARPERA, we have an increase in total net evaporation (E−P−R) over the eastern Mediterranean (Ionian plus Levantine basins) of 0.02 m.yr^{-1}, from 0.95 m.yr^{-1} in average over 1980–1987 to 0.97 m.yr^{-1} in average over 1988–1994. But if we consider only the Levantine basin, we have a decrease of 0.02 m.yr^{-1}, from 1.02 m.yr^{-1} in average over 1980–1987 to 1.00 m.yr^{-1} in average over 1988–1994. For the Aegean Sea (Figure 9d), the E−P−R flux amounts −0.59 m.yr^{-1} over 1980–1987 and −0.22 m.yr^{-1} over 1987–1994. This strong increase in the surface water loss over the Aegean Sea are in fact largely dominated by the reduction of the Black Sea inflow, from 9071 m^3.s^{-1} in average over 1980–1987 to 7530 m^3.s^{-1} over 1988–1994, which is equivalent to a decrease of this inflow from 1.63 m.yr^{-1} over 1980–1987 to 1.36 m.yr^{-1} over 1987–1994 (values relative to the surface of the Aegean Sea). Considering only the atmospheric water flux (E−P) over the Aegean Sea (Figure 9c), i.e., without taking into account the variations of the freshwater input from the Black Sea and of some minor rivers, we have an increase of the net evaporation from 1.07 m.yr^{-1} to 1.14 m.yr^{-1} for the same periods over the Aegean Sea.

[48] So it seems that the behavior of the time variations of the atmospheric flux changes from one sub-basin to another. If we come back to the eastern Mediterranean and to the range of 0.1–0.2 m.yr^{-1} given by *Roether et al.* [1996] and *Tsimplis and Josey* [2001] for change in the net evaporation, we find that 10 to 20% of the salinity increase in the eastern Mediterranean can be explained through changes in net surface freshwater flux according to the ARPERA data set. Thus the major part of this salinity increase, at least for the deep layers, must have been driven by internal salinity redistribution, as concluded by *Josey* [2003] for this point. The increase of the net evaporation rather plays a significant

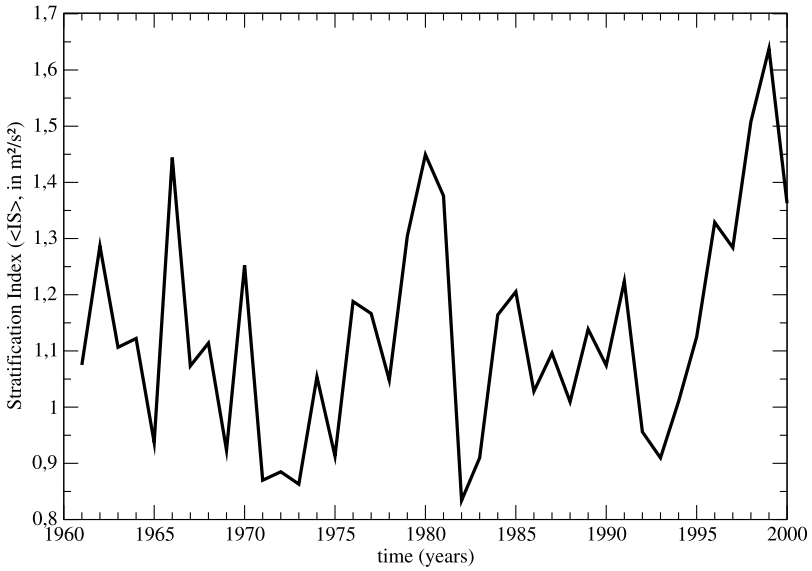

Figure 10. Monthly values of the stratification index ($\langle IS \rangle$, in $m^2.s^{-2}$), in the Aegean Sea, for NM8-atl-riv, in November for the 1961–2000 period.

role in increasing the salinity of the surface layer (as mentioned previously).

4.1.3. Changes in the Vertical Stratification of the Aegean Sea

[49] We investigate in this section the preconditioning of the convection by looking at the vertical stratification in the Aegean Sea at the beginning of winter. For that we compute for each November, just before winter of each simulated year, a vertical Index of Stratification (in $m^2.s^{-2}$ [see *Lascaratos*, 1993; *Somot*, 2005; *Herrmann et al.*, 2008]) at each model grid point (i,j) and for a given depth h, which is

$$IS(i,j,h) = \int_0^h N^2(i,j,z).z.dz,$$

with z and h depths taken positive and N (s^{-1}) the local Brunt-Vaisala frequency. With $N^2 = \frac{g}{\rho}\frac{\partial \rho}{\partial z}$ (g is the gravity and ρ the water density), it gives

$$IS(i,j,h) = g\int_0^h \frac{z}{\rho(i,j,z)}d\rho.$$

$H_{i,j}$ is taken equal to the local bottom sea depth to obtain the stratification of the whole water column at the model grid point (i,j). Thus, IS(i,j,$H_{i,j}$) represents the potential buoyancy loss needed to generate deep convection that reaches the bottom of the sea at the model grid point (i,j). This computation was applied for each Aegean grid point (i,j), characterized by its local maximal depth $H_{i,j}$, and then we averaged the values horizontally over the whole Aegean Sea to obtain a vertical index of stratification for the Aegean Sea, $\langle IS \rangle$.

[50] Figure 10 displays these monthly $\langle IS \rangle$ values in November. The lower the $\langle IS \rangle$ value is, the weaker the stratification is and the easier it is to obtain convection. In November 1992, just before the winter of interest, the Aegean Sea has a particularly low stratification; yet it is only the tenth lowest value of the 40 simulated years. $\langle IS \rangle$ values are lower only in November 1965, 1969, 1971, 1972, 1973, 1975, 1982, 1983, and 1993. We can note that this particularly low stratification in November 1992 represents a major reduction from the value in November 1991. Thus, in the time spanned by the onset of the EMT (1987–1992), the period November 1991–November 1992 has the biggest impact on the stratification in the Aegean Sea. And presumably this is due to the severe winter 1991–1992.

[51] This means that the potential preconditioning factors we mentioned before, which mainly tend to increase the salinity of the surface and intermediate layers of the Aegean Sea, have a very weak impact of the stratification of the water column before November 1991. The changes in the Levantine surface circulation, the increase of the net evaporation in the eastern Mediterranean or the decrease of the Black Sea inflow between the beginning and the end of the 1980s are indeed real but they do not destabilize the water column of the Aegean Sea. Thus, the real triggering elements of the EMT are the strong atmospheric fluxes which occurred during the winters 1991–1992 and 1992–1993.

4.2. Aegean Winter Deep Convection

[52] In this section, we first focus on the surface fluxes over the Aegean Sea. Over this area, the winters of 1991–1992 and 1992–1993 were characterized by a very cold, dry atmosphere and high winds which resulted in strong heat loss and net evaporation, as found by *Josey* [2003] on the basis of atmospheric reanalysis data. These facts are reproduced in ARPERA forcings (Figure 11). The winter heat flux anomalies (Figure 11a) during 1991–1992 and 1992–1993 present the highest heat losses over the 40 years of simulation (anomalies of −73 and −65 $W.m^{-2}$ respectively). The water flux anomalies (Figure 11b) are also very negative during winters 1989–1990 to 1992–1993, corresponding to a higher net evaporation rate. Again, the latter has the strongest water loss over the 40 years, with an anomaly of −2.8 mm. day^{-1} (−1.0 $m.yr^{-1}$). However, one has to note that the heat loss has a significant impact on the surface density while the

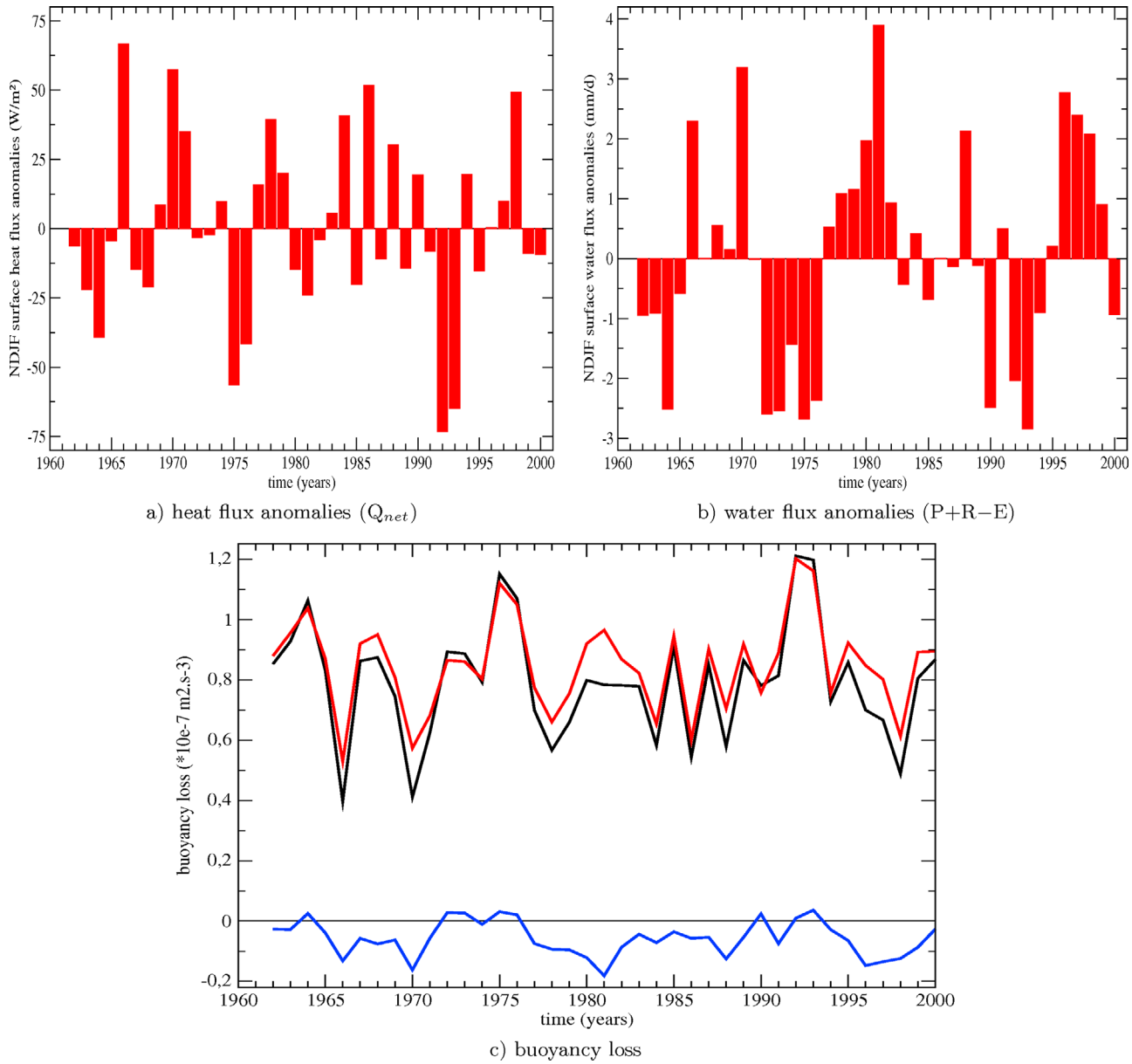

Figure 11. Anomalies of winter (NDJF) averaged surface fluxes over the Aegean Sea: (a) net heat flux anomalies (in W.m^{-2}) and (b) net freshwater flux anomalies (Precipitations+Runoff-Evaporation anomalies in mm.day^{-1}) for NM8-atl-riv. (c) Winter (NDJF) mean of the components of the surface buoyancy loss (in 10^{-7} m^2.s^{-3}) over the Aegean Sea: contribution of the heat loss (red line), contribution of the water loss (blue line), and total buoyancy loss (black line). The tick mark of the year in the time axis corresponds to January.

net evaporation (i.e., water loss) has a minor influence, as mentioned by *Josey* [2003]. This fact can be estimated by calculating, following the method of *Mertens and Schott* [1998], the parts of the buoyancy loss which are respectively caused by the heat and the water loss (Figure 11c). The averaged values for each component over the Aegean Sea in winter (NDJF) are $+8.5 \times 10^{-8}$ m^2.s^{-3} for the thermal buoyancy loss, -0.6×10^{-8} m^2.s^{-3} for the water buoyancy loss and so $+7.9 \times 10^{-8}$ m^2.s^{-3} for the total buoyancy loss. The time correlation amounts 0.97 between the thermal buoyancy loss and the total buoyancy loss, 0.73 between the water buoyancy loss and the total buoyancy loss. Thus, the heat loss is indeed the major component of the buoyancy loss in terms of mean value as well as in terms of time variations.

[53] It can be noticed on Figure 11 that similar cold winters conditions occurred around 1975, as mentioned by *Josey* [2003], and we will see in the following that deep convection also occurred during this period. Figures 12 and 13 show the evolution of the volume of dense waters in the Aegean Sea and the associated annual formation rates (red lines and bars for NM8-atl-riv). The newly formed waters are very dense (≥29.2 kg.m^{-3}), in agreement with observations of *Theocharis et al.* [1999]. The year 1993 emerges in

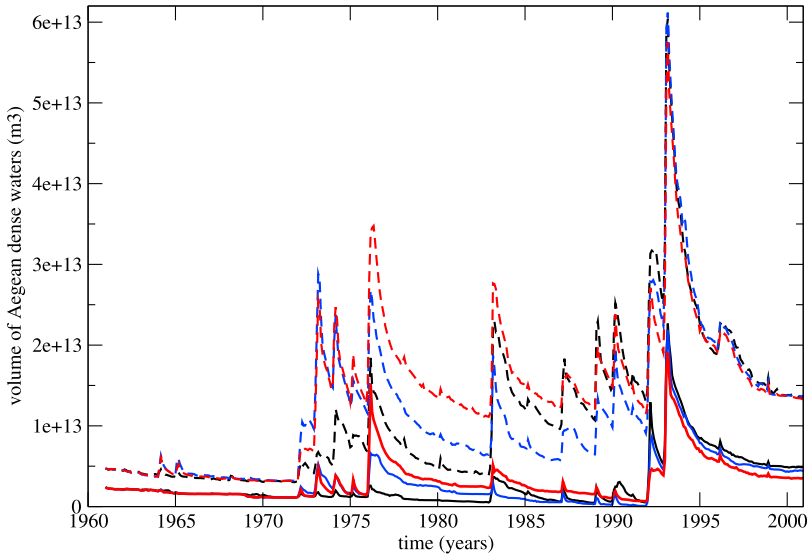

Figure 12. Monthly volume (in m^3) of Aegean waters denser than 29.2 $kg.m^{-3}$ (dashed line) and 29.3 $kg.m^{-3}$ (solid line), for the three simulations: NM8-atl-riv (red), NM8-riv (blue), and NM8-clim (black). Values for the waters denser than 29.2 $kg.m^{-3}$ include the values of waters denser than 29.3 $kg.m^{-3}$.

these two plots: indeed, in 1993 about 75% of the Aegean Sea is filled by waters denser than 29.2 $kg.m^{-3}$. The associated formation rate is also the highest over the 40 years: 1.22 Sv for the density 29.2, in which 0.48 Sv corresponds to waters denser than 29.3 $kg.m^{-3}$ (Table 6). Figures 12 and 13 also show that deep convection takes place during many winters before 1992: 1987, 1989, and 1990. The period 1972–1975 and in particular the year 1976 are noticeable too. In relation with the surface fluxes mentioned before, deep winter convection occurs between 1972 and 1976 (especially in 1976 with formation of waters denser than 29.3 $kg.m^{-3}$), but it forms during these five years a quantity of dense waters about two times lower than in 1992 and 1993. These results support the hypothesis advanced by *Josey* [2003]: the surface forcing in the period 1972–1976 produced conditions that caused deep water formation in the Aegean Sea, but with lower formation rates than in the early 1990s.

[54] *Zervakis et al.* [2000] and *Gertman et al.* [2006] argued that the EMT started in 1987 with dense water formation in the northern Aegean Sea. *Theocharis et al.* [1999] reported that CDW was observed in March 1987 in the Cretan Sea and started to exit the Aegean Sea in 1989, at intermediate depths for a first time. These observations indicate that the EMT is not a phenomenon localized in time, but rather a continuously evolving process during the period 1987–1995. Indeed, the Aegean Sea is steadily filled with dense waters which are produced locally during many winters: 1987, 1989, 1990, 1992, and 1993 (Figures 12 and 13). Meridian sections of density in the Aegean Sea illustrate the increase in density of the Aegean Sea, from north to south and from 1970 to 1993 (Figure 14), in agreement with *Zervakis et al.* [2000]. The changes between 1970 (Figure 14a) and 1980 (Figure 14b) show that during the decade of the 1970s, waters denser than 29.2 $kg.m^{-3}$ have filled the bottom layers of the northern, central and southern sub-basins of the Aegean Sea. Then, until 1992, the central and northern sub-basins have been continuously filled with denser waters below 200 m depth (Figures 14c–14e), whereas the southern sub-basin (Cretan Sea) has been filled by waters of lower density (uplift of the 29.1 isopycnal surface but sinking of the 29.2 isopycnal surface between 1987 (Figure 14c) and 1992 (Figure 14e)). In 1993, the huge increase of the volume of dense waters during one single winter (see Figure 12) is due to the production of dense waters in the Cretan Sea (Figure 14f). As the volume of the Cretan Sea exceeds the volume of the other Aegean sub-basins, its filling by dense waters has a higher signature in Figure 12 which corresponds to the total volume of Aegean dense waters.

[55] As we did for the whole Mediterranean Sea (Figure 6), we are going to compare the results of the simulations in the Aegean Sea with the interannual gridded database of *Rixen et al.* [2005]. It is important to keep in mind that there are few available observations of salinity in this area, especially in the deep layer; in these cases, it will be hard to say which of the model or the database is the closest to reality. Figure 8 displays the Aegean heat and salt contents. As in section 3.3, the heat content evolution is better reproduced than the salt content one, as confirmed by the temporal correlations (see Table 5). But we can notice that the variations of the simulated salt content in the Aegean Sea have the same amplitudes with the observed ones, which is better than for the global Mediterranean basin. The variations of the salt content in the Aegean Sea are influenced by the different strategies used for modeling the Black Sea input. We will focus more precisely on that point in the section 4.4. Here we focus on the NM8-atl-riv simulation (red lines in Figure 8).

[56] The variations of the temperature are well reproduced in the surface and intermediate layers of the Aegean Sea, despite a slight cold bias in the surface and a warm bias more or less pronounced in time for the intermediate layer. The variations of the salinity in the surface layer are strongly influenced by the variations of the Black Sea input, presented in Figure 3. When this runoff is weaker than the

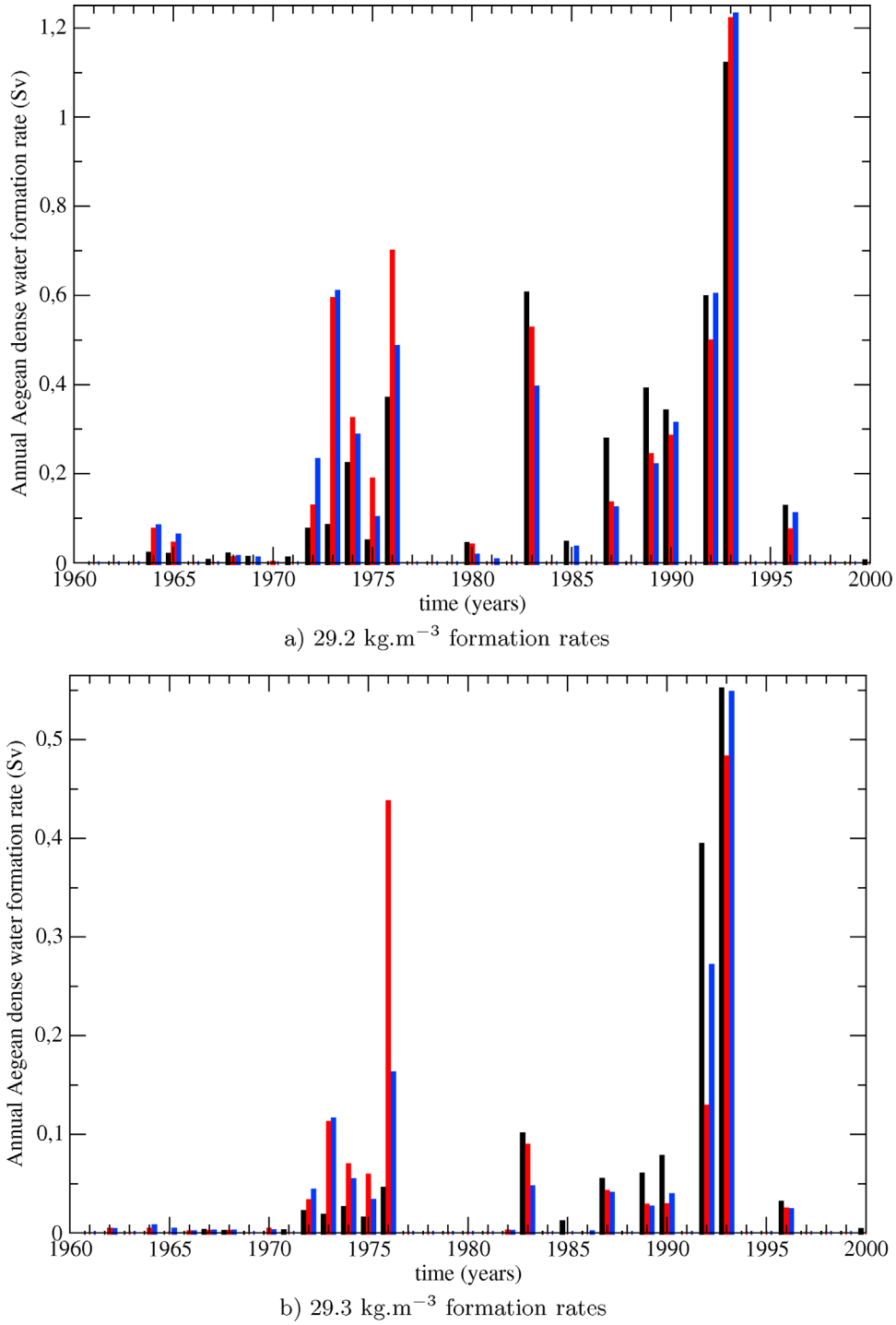

Figure 13. Annual formation rate (in Sv) of dense waters in the Aegean Sea, for the three simulations, NM8-atl-riv (red), NM8-riv (blue), and NM8-clim (black), for two thresholds: (a) 29.2 kg.m^{-3} and (b) 29.3 kg.m^{-3} (vertical scales differ between Figure 13a and Figure 13b). Values for some years are given in Table 6.

climatological value (mainly in the early 1960s and 1970s), we can see a higher salt content in the Aegean surface layer, leading to a favorable preconditioning of the convection. Conversely, when the Black Sea input is stronger than the climatological value (around 1970, in the early 1980s and late 1990s for example), it leads to a decrease of the Aegean surface salt content.

[57] The evolution of the intermediate and deep salt contents in Figure 8 show variations that can be linked to the occurrence of winter convection in general (see Figure 12) and of the EMT in particular. As mentioned by *Theocharis*

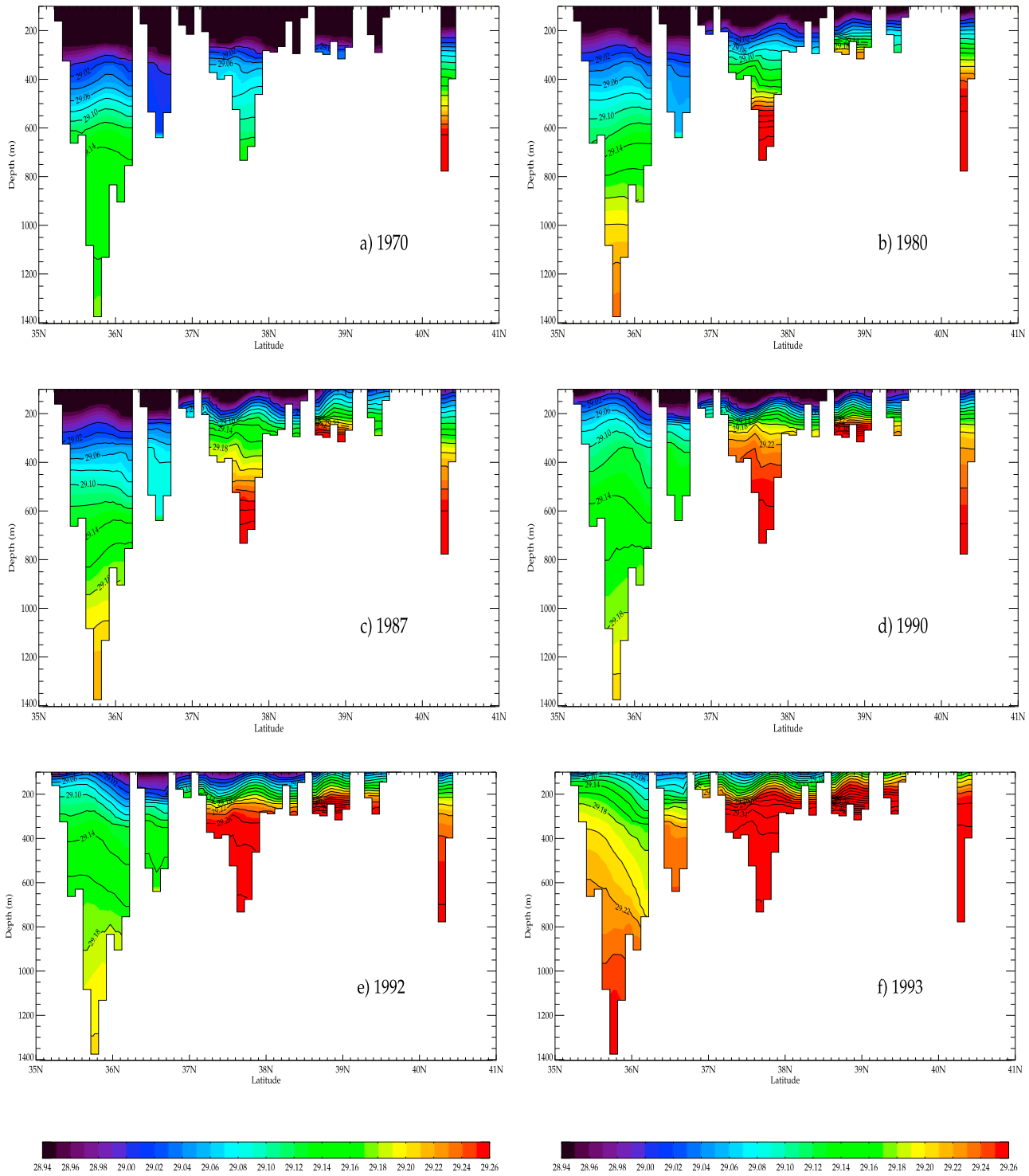

Figure 14. Meridian sections of potential density (in kg.m^{-3}) across the Aegean Sea at 25.8°E, from 100 m to 1400 m depth (section A in Figure 1). Annual means in the simulation NM8-atl-riv in (a) 1970, (b) 1980, (c) 1987, (d) 1990, (e) 1992, and (f) 1993. Contour lines are drawn from 29.00 kg.m^{-3} to 29.60 kg.m^{-3} with interval of 0.02 kg.m^{-3}.

et al. [1999], the signature of the EMT corresponds to a temperature drop in 1992–1994 and to a salinity increase between 1987 and 1992. In the simulation, the temperature drop is obvious in all layers, the salinity increase is mainly visible for the intermediate and bottom layers as for the averaged water column. In the early 1970s and in the early 1990s, when the convection is strong and reaches high depths, the water column is homogenized and becomes warmer and saltier, especially in the deep layers (Figures 8g and 8h). But in 1992 and 1993, due to the strong atmo-

Table 5. Characteristics of the Three Simulations Over 1961–2000: Heat and Salt Content for Different Layers of the Aegean Sea[a]

	Mean Over 1961–2000				Mean Bias			Correlation		
	atl-riv	riv	clim	Rixen	atl-riv	riv	clim	atl-riv	riv	clim
Heat content (in °C)										
Total	15.03	15.04	15.05	14.70	+0.33	+0.34	+0.35	0.79	0.82	0.82
0–150 m	16.31	16.32	16.31	16.57	−0.26	−0.25	−0.26	0.75	0.76	0.78
150–600 m	14.68	14.69	14.74	14.47	+0.21	+0.22	+0.27	0.73	0.65	0.63
600 m–bottom	14.18	14.19	14.15	13.70	+0.48	+0.49	+0.45	n.s.	n.s.	n.s.
Salt content (in psu)										
Total	38.87	38.87	38.87	38.83	+0.04	+0.04	+0.04	0.38	0.43	0.63
0–150 m	38.68	38.68	38.68	38.75	−0.07	−0.07	−0.07	0.40	0.44	0.67
150–600 m	38.94	38.94	38.95	38.90	+0.04	+0.04	+0.05	n.s.	0.35	0.39
600 m–bottom	38.95	38.94	38.93	38.81	+0.15	+0.14	+0.13	n.s.	n.s.	n.s.

[a]Here n.s. means "non-significant," the value is inside the ±1 standard deviation of the interannual gridded database of *Rixen et al.* [2005]. The given correlations are computed after removing trends, for both the simulations nM8- and the database of *Rixen et al.* [2005]. Significant correlations are those with values outside the 95% confidence interval (significantly different from zero if the absolute value of the correlation is larger or equal than 0.31).

spheric cooling over the Aegean Sea, a negative surface temperature anomaly is brought towards the deeper layers. That is why during the convection events of 1992 and 1993 there is a decrease in temperature of the deep layers instead of an increase like in the 1970s.

4.3. Outflow and Spreading of Aegean Dense Waters

[58] The Aegean Sea was gradually filled by dense waters during several convective winters. In 1993, the volume of Aegean waters denser than 29.2 kg.m^{-3} corresponds to 75% of the volume of the Aegean Sea. During this year, an increase of the density of the waters inside the Cretan Sea was observed, with maximal value of 29.4 kg.m^{-3} at particular sites [*Theocharis et al.*, 1999]. In the simulation, the potential density only reaches the maximal value of 29.3 kg.m^{-3} in April 1993 near the bottom of the Cretan Sea. This Cretan Deep Water (CDW) tends to exit the Aegean Sea through three straits of the Cretan Arc (Antikithira, Kassos and Karpathos, from West to East), which link the Aegean Sea with the Ionian and the Levantine basins (see Figure 1 for their location). To follow this outflow, we compute the monthly evolution of the potential density of the waters above the sill of these straits in the model and compare it with the values of the outflow estimated with observations in the channels south of these sills (Figure 15). As the sill of the Karpathos Strait is deeper (777m in NEMOMED8) than the sill of the two others (around 540m), the density above this sill is obviously higher during the 40 years. We can here mention that in reality the Kassos Strait has a deeper sill than the Karpathos Strait (respectively 1000m and 850m according to *Kontoyiannis et al.* [2005]). This explains why observations are available for the Antikithira and Kassos straits at higher depths than in the model. The successive convection events are highlighted by the density maxima during the months following the convection (from 1973 to 1976, in 1983, 1992 and 1993). But, again, the year 1993 is distinguished among the 40 simulated

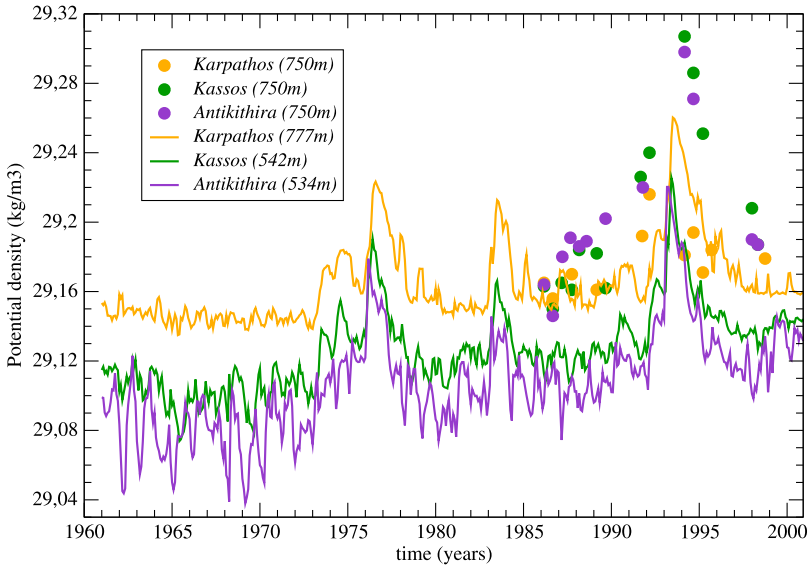

Figure 15. Monthly potential density (in kg.m^{-3}) simulated on the bottom of the Cretan Arc straits (lines) and observed just south of the sill channels (circles): Karpathos (yellow), Kassos (green), and Antikithira (purple), in the simulation NM8-atl-riv. The depth of each sill in the model and of each measurement is indicated in parentheses.

years, giving the highest density of the 1961–2000 period (≥29.22) above the three sills during the first months of 1993. The density maximum is reached in April 1993 in the Antikithira Strait (29.220 kg.m^{-3}), in June 1993 in the Kassos Strait (29.226 kg.m^{-3}) and in July 1993 in the Karpathos Strait (29.260 kg.m^{-3}). So, the densest waters first exit through the western straits of the Cretan Arc and afterwards through the eastern straits: it can be linked to the cyclonic circulation inside the Cretan Sea. If compared to the observations, the results are in good agreement for the Karpathos Strait (solid line and circles in Figure 15) because both observations and simulations are at the same depth. In fact, the agreement is excellent between 1986 and 1990 and then the increase observed in 1992 is underestimated in the model. This can be linked to the fact that only a density of 29.3 kg.m^{-3} is reached at the bottom of the Cretan Sea rather than 29.4 kg.m^{-3} in the observations. Of course, as the Antikithira and Kassos straits are shallower in the model than in reality, the steady increase and the maximum of density observed for theses two straits are shifted towards lower values in the model. However, the general behaviour is correctly reproduced, i.e., there is a simulated density increase of 0.12 kg.m^{-3} for the Antikithira Strait between 1988 and the peak-value of 1993 (against 0.14 kg.m^{-3} in the observations) and a corresponding simulated increase of 0.11 kg.m^{-3} for the Kassos Strait (against 0.15 kg.m^{-3} in the observations). Moreover, we want to mention that there is no available observation of this dense outflow between 1992 and 1994; thus, the modeling can here play the role of a new source of information about the description of the sequence of the EMT events during this period for which observations lack. One can suppose that a peak in density, higher than the observed value of 29.31 kg.m^{-3} in winter 1994, occurred during fall 1993 and possibly reached even higher values at this time, as suggested by the results of the simulation.

[59] Then, because we do not simulate a sufficient increase of the potential density inside the Cretan Sea, the volume of dense waters which exit the Aegean Sea is underestimated with regards to observations. Table 7 displays the annual averaged dense outflow rates. For the simulation NM8-atl-riv, the outflow of dense waters (threshold 29.2 kg.m^{-3}) occurs only in 1993 through both the western and eastern straits of the Cretan Arc and in 1994 only through Karpathos Strait. Same outflow locations are obtained with a lower threshold of 29.19 kg.m^{-3}. It indicates that 0.31 Sv of waters outflow with a density between 29.19 and 29.20 kg.m^{-3}. Lowering the threshold to 29.18 kg.m^{-3}, we notice that the outflow persists in 1995 through the Karpathos Strait. 0.55 Sv of waters outflow with a density ranged between 29.18 and 29.19 kg.m^{-3}. The total outflow for this latter threshold amounts 1.39 Sv. This value is two times lower than the total outflow of 2.8 Sv estimated between mid-1992 and the end of 1994 from observations [*Roether et al.*, 2007].

[60] After exiting the Aegean Sea through the Cretan Arc straits, this dense CDW mass overflowed and was mixed in the Ionian and the Levantine basins [*Roether et al.*, 2007]. Figure 16 displays the depth and the salinity of the 29.165 kg.m^{-3} isopycnal surface during and after the simulated EMT. We take this relatively low density value because of the mixing that affects the CDW in the eastern Mediterranean. The waters going through Antikithira Strait in the Ionian basin first spread at low depths (around 200 m depth in Figure 16a) and then sink. They turn in a cyclonic manner and they flow north-westwards following the shelf slope. The waters exiting the Aegean Sea east of Crete at shallow depths through Kassos and Karpathos straits (around 400 m depth in Figure 16a), spread in the Levantine basin and sink. A part of them turns westwards through the Cretan Passage (Figures 16b and 16c) and joins the waters exiting from Antikithira Strait (in agreement with *Roether et al.* [2007]). Another part remains inside the Levantine basin (east of 24°E). Their path is first southwards before becoming cyclonic along the shelf slope of the Levantine basin (Figures 16c and 16d). Finally, a small part of waters propagates eastwards from the Karpathos Strait, mainly driven by diffusive processes or carried by deep eddies (Figure 16c at 30°E for example). We notice that the sinking of CDW in the Ionian and Levantine basins has two effects: first the uplift of this 29.165 isopycnal surface by at least 400 meters, from 1600 m depth in 1993 before the EMT (Figure 16a) to 1200 m depth in 2000 at the end of the simulation (Figure 16d), secondly the salt increase of the eastern Mediterranean at these depths, from 38.70 psu in 1993 to 38.79 psu in 2000. This simulated salt increase has the same amplitude as the observed one between the pre-EMT period and 2001 [*Roether et al.*, 2007].

[61] Figure 17 shows the salinity on the 29.18 kg.m^{-3} isopycnal surface and the bathymetry in the Levantine basin. The Antikithira and the Kassos straits have a shallower sill than the Karpathos Strait in the model. This explains why the volume of CDW at this density, which exits the Aegean Sea, is particularly huge through the Karpathos Strait (Figure 17b). Once in the Levantine basin, this water mass rapidly sinks below and east of the sill of the Cretan Passage (located at about 2000 m depth, 24.5°E 34.5°N) and thus spreads inside the Levantine basin. Mixing processes with surrounding waters of lower density make it difficult to find the signature of these denser waters after 1995 (Figure 17c). However, we notice that in 2000 the water mass corresponding to this density flows along the southern shelf slope of the Levantine basin along the 2250 m isobath in Figure 17d.

[62] The core of the outflowing CDW tongue has thermohaline characteristics of 13.9°C and 38.85 psu in January 1995 (at 2000m depth), which is 0.3°C warmer and 0.05 psu saltier than the one observed at this time [*Klein et al.*, 1999]. This can be related to the warm and salty bias in the intermediate layer throughout the studied region. Besides, the densest part of the CDW in the eastern Mediterranean only reaches the depth of about 2500 m in the simulation (not shown), whereas it sinks to the bottom of the Ionian and Levantine basins according to observations of *Klein et al.* [1999]. Three explanations could be proposed. First, the density of the simulated CDW is too low with regard to the observations (as mentioned previously). Secondly, the mixing in the oceanic model is too strong due to its resolution and need to be better parameterized. Indeed, the decrease of the CDW volume once in the Levantine and Ionian basins is too quick (the density of the CDW is 29.182 kg.m^{-3} at around 2200m depth in January 1995), although the CDW overflows through Antikithira and Kassos straits with a density higher than 29.22 kg.m^{-3} and through the Karpathos Strait with a density higher than 29.26 kg.m^{-3} in the model (Figure 15). Thirdly, the simulated CDW is less dense than the resident bottom waters of the model (around 29.2 kg.m^{-3}), related to

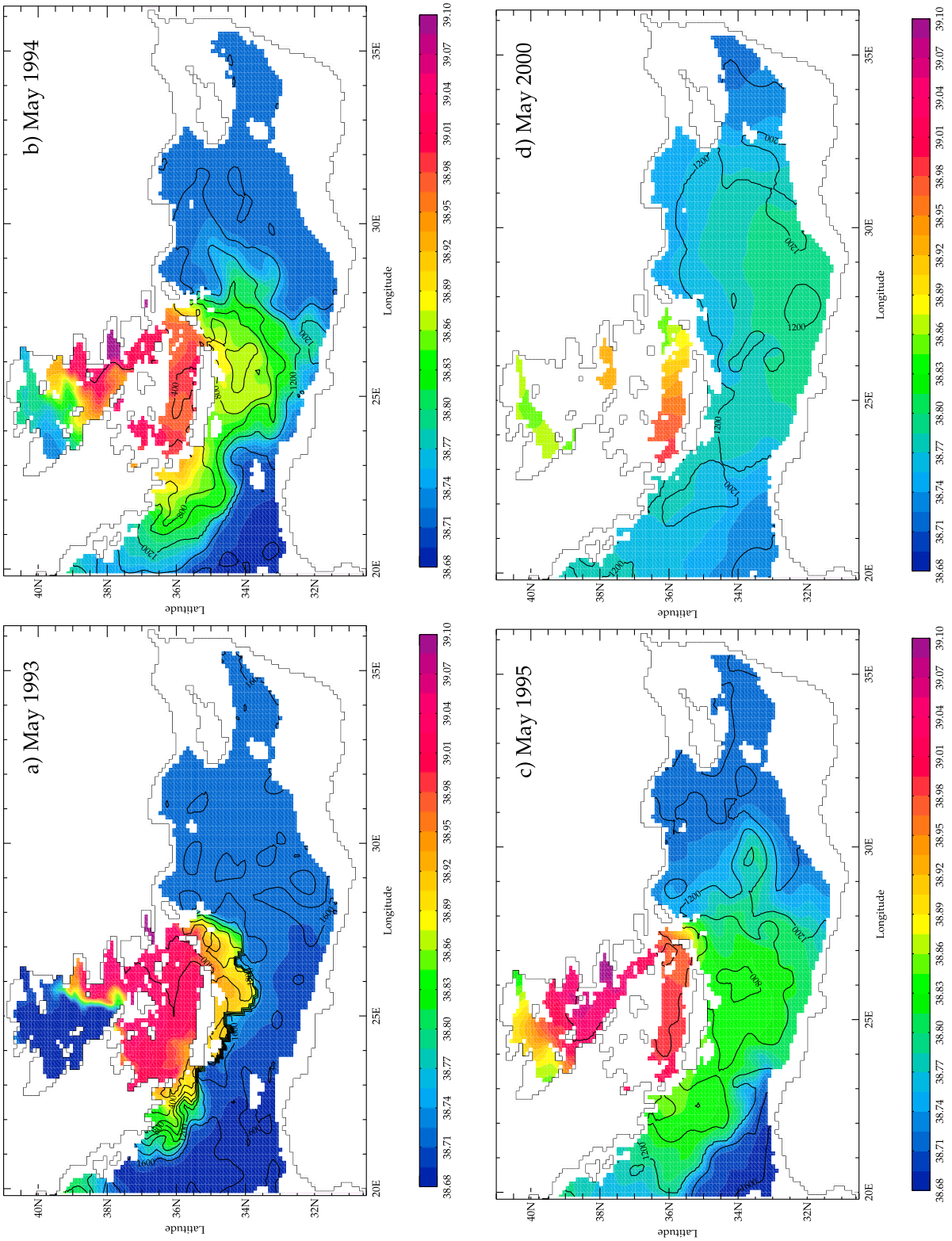

Figure 16. Maps of the isopycnal surface $\sigma_\theta = 29.165$ kg.m^{-3}: depth of this surface (contour lines, interval of 200 m) and salinity on this surface (colors, interval of 0.015 psu). Model outputs for NM8-atl-riv in May (a) 1993, (b) 1994, (c) 1995, and (d) 2000.

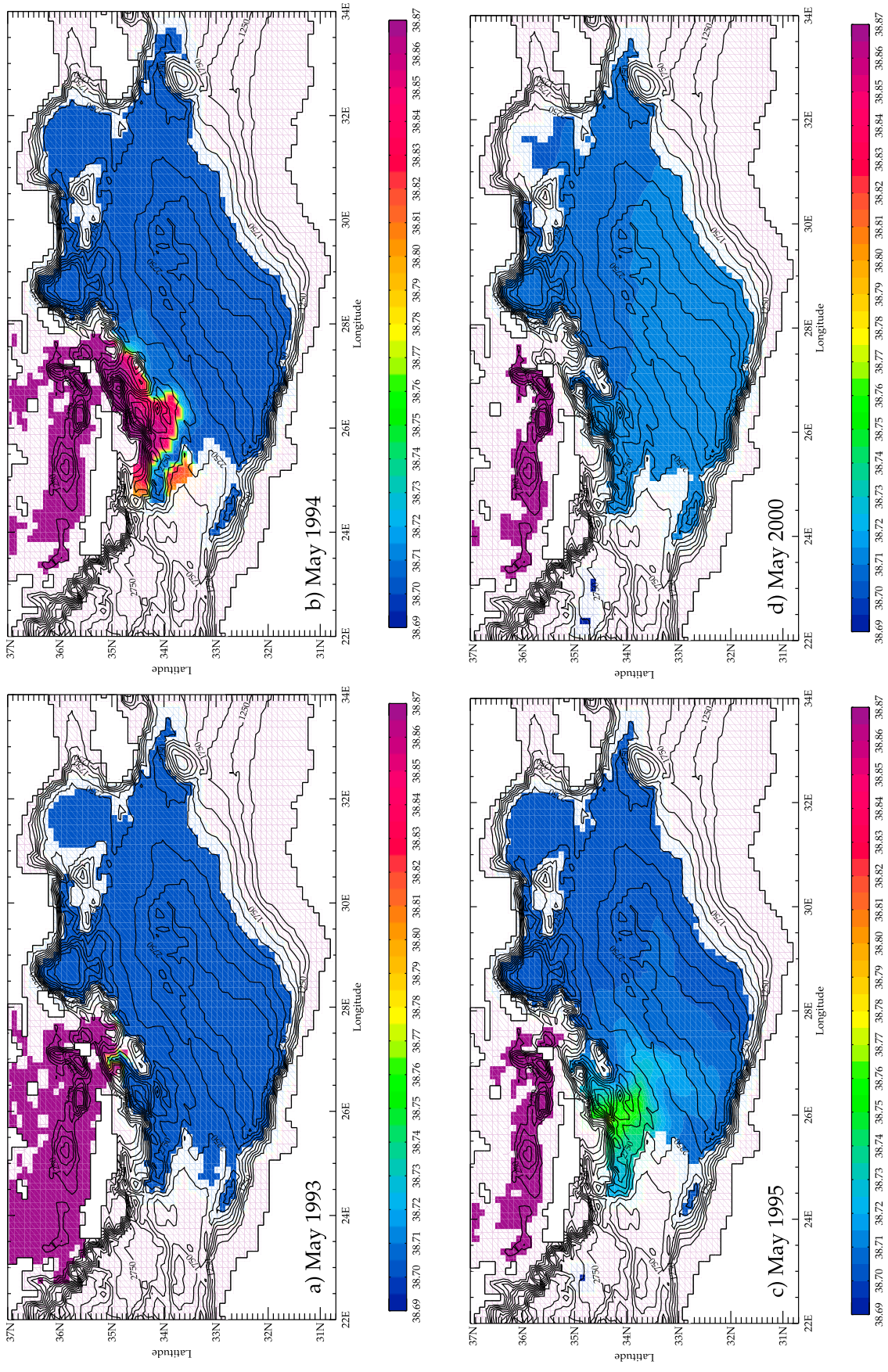

Figure 17. Salinity (colors, interval of 0.005 psu) on the isopycnal surface σ_θ = 29.18 kg.m^{-3} and bathymetry (contour lines, interval of 250 m from 1000 m to 4000 m depth). Model outputs for NM8-atl-riv in May (a) 1993, (b) 1994, (c) 1995, and (d) 2000.

Table 6. Annual Dense Water Formation Rates for the Aegean Sea for the Three Companion Simulations and for the 29.2 and 29.3 kg.m^{-3} Density Thresholds[a]

	1971–1978		1983–1990		1992		1993	
Simulation	≥29.2	≥29.3	≥29.2	≥29.3	≥29.2	≥29.3	≥29.2	≥29.3
NM8-atl-riv	0.24	0.09	0.15	0.02	0.50	0.13	1.22	0.48
NM8-riv	0.21	0.05	0.13	0.02	0.60	0.27	1.23	0.55
NM8-clim	0.10	0.02	0.21	0.04	0.60	0.39	1.12	0.55

[a]Annual dense water formation rates are given in Sv.

the initial state of the MEDATLAS climatology, whereas they were observed at 29.17 kg.m^{-3} in 1987 before the EMT [*Roether et al.*, 2007]. So this modeled CDW can not sink to depths greater than the depths of the resident waters, i.e., to the bottom of the eastern Mediterranean. Thus, despite room for improvement still clearly exists, the model, which is driven by realistic atmospheric and hydrological forcings, has reproduced strong convection events in the Aegean Sea following by a huge outflow of dense CDW in the eastern Mediterranean.

4.4. Influence of the Interannual Variations of the River Runoffs

[63] The effects of interannual river runoffs on the modeling of the convection in the Aegean Sea, in particular during the EMT, are here investigated. As the variations of the Black Sea input are higher than those of any other Mediterranean "river," especially when one focuses on the Aegean Sea [*Zervakis et al.*, 2000], the comparison between the simulations NM8-clim and NM8-riv will point out the impact of the Black Sea. *Zervakis et al.* [2000] argued that the decrease of the Black Sea input in the early 1990s was an important element in the triggering of the EMT. However, the values of the interannual Black Sea discharge in the early 1990s in our interannual data set are close to the climatological value: the differences between the red solid and dashed lines in Figure 3 are small between 1989 and 1992 and represent less than 10% of the annual climatological value. As a consequence, the maximal amount of dense waters produced in the Aegean Sea in 1993 is slightly the same in the two simulations NM8-clim and NM8-riv. The difference in 1993 is less than 1%, as shown by the black and blue dashed lines in Figure 12. As for the NM8-atl-riv simulation (see section 4.2), the volume of water denser than 29.2 kg.m^{-3} in 1993 still corresponds to about 75% of the total volume of the Aegean Sea in the two other simulations. Table 6 highlights that NM8-clim and NM8-riv have the same rates of dense water formation in 1992 for the 29.2 density threshold and in 1993 for the 29.3 density threshold. Although NM8-clim forms 0.12 Sv more of waters denser than 29.3 kg.m^{-3} in 1992 and NM8-riv forms 0.11 Sv more of waters denser than 29.2 kg.m^{-3} in 1993, the Aegean Sea is filled by the same amount of dense waters in 1993 for these simulations. This is confirmed by the outflow values for waters denser than 29.2 kg.m^{-3} (Table 7). Nevertheless, if we lower the threshold, the water volume which outflows is higher and the export lasts longer (until 1996) in NM8-clim than in NM8-riv. Among the 2.70 Sv that outflow between 1992 and 1996 in NM8-clim (2.08 Sv in NM8-riv), 1.38 Sv have a density ranged between 29.18 and 29.19 kg.m^{-3} (0.85 Sv) and 0.56 Sv between 29.19 and 29.20 kg.m^{-3} (0.42 Sv). But a 2.70 Sv total outflow in 5 years, between 1992 and 1996, corresponds to a weak outflow of dense waters if compared to the 2.80 Sv observed in 2.5 years, between mid-1992 and the end of 1994 [*Roether et al.*, 2007].

[64] In fact, the difference between these two experiments concerning the convection in the Aegean Sea is more substantial in the 1970s and in the 1980s. It corresponds to periods during which the variations of the interannual Black Sea discharge are high and reach 75% of the annual climatological value. The lowest Black Sea input during the 1961–2000 period is reached in 1972 (2626 m^3.s^{-1}) and the highest one is reached in 1980 (13981 m^3.s^{-1}). In particular, during the 1971–1976 period, the Black Sea input was very low during many consecutive years (−40% in average during this 6-year period, see Figure 3). As a result, 0.11 Sv more of waters denser than 29.2 kg.m^{-3} and 0.03 Sv more waters denser than 29.3 kg.m^{-3} are formed in NM8-riv compared to NM8-clim in average over eight years, from 1971 to 1978 (Table 6). Conversely, NM8-clim forms about 0.08 Sv more waters denser than 29.2 kg.m^{-3} and 0.02 Sv more waters denser than 29.3 kg.m^{-3} during the eight-year period of 1983–1990.

Table 7. Annual Dense Outflows Through the Western and the Eastern Cretan Arc Straits[a]

	1992		1993		1994		1995		1996		Total
Simulation	W	E	W	E	W	E	W	E	W	E	W + E
Outflow ≥ 29.20 kg.m^{-3}											
NM8-atl-riv	0	0	0.02	0.42	0	0.09	0	0	0	0	0.53
NM8-riv	0	0	0.02	0.57	0	0.22	0	0	0	0	0.81
NM8-clim	0	0	0.11	0.51	0	0.14	0	0	0	0	0.76
Outflow ≥ 29.19 kg.m^{-3}											
NM8-atl-riv	0	0	0.02	0.59	0	0.23	0	0	0	0	0.84
NM8-riv	0	0	0.11	0.80	0	0.32	0	0	0	0	1.23
NM8-clim	0	0.03	0.25	0.80	0	0.24	0	0	0	0	1.32
Outflow ≥ 29.18 kg.m^{-3}											
NM8-atl-riv	0	0	0.19	0.84	0	0.33	0	0.03	0	0	1.39
NM8-riv	0	0.15	0.34	0.98	0	0.47	0	0.13	0	0.01	2.08
NM8-clim	0.01	0.25	0.94	0.98	0.02	0.35	0	0.10	0	0.05	2.70

[a]Annual dense outflows are given in Sv. The western and the eastern Cretan Arc straits are Antikithira, W and Kassos and Karpathos, E, respectively. Values for water denser than different thresholds. These values are obtained as yearly averages of monthly dense outflow values.

[65] If we look at the thermohaline characteristics of the Aegean Sea in basin average (Figure 8), the first noticeable difference between NM8-riv (blue lines) and NM8-clim (black lines) concerns the salt content of the surface layer. It is indeed strongly influenced by the interannual variations of the Black Sea discharge introduced in NM8-riv. The second important change concerns the heat and salt contents of the deep layer (600 m-bottom) in the 1970s. The amount of dense water formed (Figures 12 and 13) is larger in NM8-riv (blue lines and bars) than in NM8-clim (black lines and bars), causing a stronger warming and a salt increase of the waters in this deep layer (Figures 8g and 8h) in NM8-riv (blue) than in NM8-clim (black). Inversely, during the 1982–1989 period, the heat content and particularly the salt content decreased in the deep layer of NM8-riv (due to the absence of deep convection and thus mixing during this period) whereas they increased in the deep layer of NM8-clim. During the EMT period, the heat and salt contents both show the same variations, with a slightly higher salinity in NM8-clim.

[66] In conclusion, the interannual variations of the Black Sea input do not play a major role on triggering the EMT in our simulations, because of close values of the Black Sea discharge in the interannual and climatological data sets during the early 1990s. The high variations of the interannual Black Sea discharge rather affect the intensity of the convection in the Aegean Sea during the previous decades. It is obvious that the convection is enhanced in the 1970s and weakened in the 1980s (when NM8-riv is compared to NM8-clim). We can mention here that our data set for the Black Sea inflow is an indirect measurement since it is deduced from the E−P−R budget of the Black Sea. Direct observed values at the Dardannelles Strait would be better, but they are not available for a long period of time.

4.5. Influence of the Interannual Variation of the Atlantic Waters

[67] In this section, we try to quantify the possible effects of the interannual variations of the Atlantic thermohaline characteristics on the representation of the convection in the Aegean Sea, with a focus on the EMT. We thus compare the NM8-riv and NM8-atl-riv simulations, which differ in using respectively a seasonal climatology and an interannual data set in the Atlantic buffer zone (Figure 2). It should be noted that at least one to two years are required for the AW anomalies to reach the far eastern Mediterranean.

[68] During the EMT period, the maximum filling of the Aegean Sea by dense waters in 1993 is slightly lower in NM8-atl-riv by about 6% than in NM8-riv (see the blue and red dashed lines in Figure 12). In 1992, the volume of dense waters formed with a density larger than 29.2 kg.m^{-3} is 0.1 Sv lower in NM8-atl-riv than in NM8-riv, whereas in 1993 the same amount of these waters is formed in both simulations (see also Table 6). Differences are however noticed for waters of density higher than 29.3 kg.m^{-3}. A smaller amount of formed waters (0.14 Sv less in 1992 and 0.07 Sv less in 1993) have a density larger than 29.3 kg.m^{-3} in NM8-atl-riv than in NM8-riv. That indicates a slight decrease in the averaged density of the Aegean Sea, which can be related to the negative salinity anomalies introduced in the buffer zone from 1986 to 1990. This induces a lower volume of CDW dense outflow towards the eastern Mediterranean in NM8-atl-riv if compared to NM8-riv (Table 7).

[69] On the contrary, during the 1970s and the 1980s, positive anomalies of AW salinity have been introduced in the buffer zone. During these periods, the rate of dense water formation in the Aegean Sea was slightly higher for NM8-atl-riv than for NM8-riv (Table 6), in particular for water denser than 29.3 kg.m^{-3} in average over the 8-year period 1971–1978. This is mainly due to the 1976 event, which forms in NM8-atl-riv 0.70 Sv of waters denser than 29.2 kg.m^{-3} (against 0.48 Sv in NM8-riv) and 0.44 Sv of waters denser than 29.3 kg.m^{-3} (against 0.16 Sv in NM8-riv).

[70] In conclusion, the interannual variations of the AW thermohaline characteristics impact the density distribution of the waters formed during the EMT. Again, the convection in the Aegean Sea during the 1970s decade is more influenced by these changes in the AW thermohaline characteristics, especially in 1976.

5. Conclusion and Outlook

[71] In this work, we have studied the Mediterranean interannual variability and in particular the Eastern Mediterranean Transient, by using NEMOMED8, an eddy-permitting Mediterranean OGCM at 1/8° of resolution (about 10 km). A realistic hindcast was performed from 1961 to 2000, forcing the model with daily atmospheric fluxes produced with ARPERA, a dynamical downscaling of the ERA40 reanalysis. Different data sets (interannual or climatological) were used to represent the hydrological fluxes of the river runoff, the Black Sea discharge and the Atlantic Water characteristics, in addition to the freshwater flux from the atmosphere. Three companion simulations, with different data sets for these hydrological fluxes but with the same interannual atmospheric fields, were carried out. These three hindcast simulations have been validated by comparing heat and salt contents at basin-scale with respect to the interannual gridded database of *Rixen et al.* [2005]. We focused then on the most realistic simulation, the one using all the interannual hydrological databases.

[72] We have shown that this simulation was able to reproduce the sequence of the EMT events in very good agreement with the following observations: (1) the strong heat and water losses at the surface of the Aegean Sea during the winters 1991–1992 and 1992–1993 (respectively −73 W.m^{-2} and −2.0 mm.day^{-1} in NDJF 1991–1992, −65 W.m^{-2} and −2.8 mm.day^{-1} in NDJF 1992–1993); (2) the strong winter convection in the Aegean Sea triggered by these strong atmospheric fluxes (1.22 Sv of waters denser than 29.2 kg.m^{-3} formed in 1993, in which 0.48 Sv are denser than 29.3 kg.m^{-3}); (3) the huge outflow of dense waters from the Aegean Sea to the Ionian and Levantine basins through the Cretan Arc straits, especially through the eastern part (Kassos and Karpathos straits) during the two years following the intense convection event; and (4) the spreading of this water mass in the eastern Mediterranean, with a scheme of the path followed by this dense water mass from 1993 to 2000: the waters exiting the Aegean Sea through the western straits of the Cretan Arc spread in a cyclonic manner in the Ionian Sea; the waters exiting the Aegean Sea through the eastern straits of the Cretan Arc spread in the Levantine basin: a part of them crosses the Cretan Passage and joins the waters

outflowing from the western straits while another part sinks at deeper levels in the Levantine basin. That part first spreads southwards following the bathymetry in a cyclonic manner and also propagates eastwards mainly driven by diffusive processes or trapped by eddies.

[73] Among the preconditioning hypotheses (the processes which took place before 1991) proposed in the literature, we found in the simulations that (1) the surface circulation was modified in the late 1980s and the early 1990s, changing the AW path in the Levantine basin; combined with a period with net reduced freshwater inputs over the far eastern Mediterranean which induces a salt increase of the surface layer in this area, this led to a salt increase of the Aegean Sea through a saltier Asia Minor Current; (2) the three anticyclonic eddies observed in 1991 play a role in deviating and trapping the AW in the Levantine basin, rather than the LIW as mentioned in the literature, whereas those eddies are not reproduced at the observed locations; (3) there was no huge decrease of the Black Sea freshwater discharge during the early 1990s according to our interannual data set; and (4) several convection events in winters 1987, 1989, and 1990 took place before the major events of winters 1992 and 1993; they induced a steady filling of the Aegean Sea by the dense waters formed during these winters.

[74] But the major conclusion here is that all these preconditioning factors tend to increase the salt content of the Aegean Sea but they do not lead to a decrease of the vertical stratification of the Aegean Sea. The key triggering elements of the EMT are thus the surface heat and water losses which occurred during the severe winters 1991–1992 and 1992–1993.

[75] In addition, this 40-year simulation allowed us to identify the years 1972 to 1976 as another period during which atmospheric and hydrological forcings were conducive to deep water formation, but with lower formation rates and thus without significant signature of Aegean dense waters in the adjacent sub-basins.

[76] Sensitivity tests were done by using different strategies for the modeling of the hydrological fluxes. The interannual variations of the Black Sea discharge in the surface layer of the northern Aegean Sea do not influence the trigger of the EMT, but rather impact the chronology of the convection event during the previous decades, with an intensification in the 1970s and a weakening in the 1980s. The interannual variations of the AW characteristics do not change the total amount of dense waters formed in the Aegean Sea during the EMT but modify the distribution of the density of these waters; the changes in the AW thermohaline characteristics have a higher impact on the convection in the Aegean Sea during the 1972–1976 period.

[77] In the future, some technical improvements of the simulations are planned in order to better reproduce some EMT characteristics with regard to available observations. To avoid too dense waters on the bottom eastern Mediterranean at the beginning of the simulations, which prevent the CDW outflow from reaching these bottom layers during the years following the EMT, we want to start the experiments from a reanalyzed state of the Mediterranean Sea at the time of the beginning of the experiment (in our case in 1960) rather than from a climatology. Moreover, the spin-up phase of the simulations has to be improved, in order to avoid a too high heat content of the intermediate layer at the beginning of the 40-year simulations. Modifications of the parametrization of the horizontal diffusion or of the vertical mixing could act on the residence time of the CDW in the Aegean Sea, avoiding a too quick decrease of its density. Using an isopycnal diffusion or the so-called BBL (bottom boundary layer parametrization, like the work of *Stratford and Haines* [2000] for the Otranto Strait) may improve the sinking and the spreading of the CDW towards the eastern Mediterranean, as for any other water mass in the model. Using an open boundary at Dardannelles Strait would allow us to study, on the top of the variations of the Black Sea freshwater inflow, the impact of the variations of the temperature and salinity of this inflow on the modeling of the Aegean convection.

[78] Future work will then focus on the possible impact of the EMT on the western Mediterranean (by running simulations until present), on the influence of running our model in a fully two-way-coupled mode (which will incidentally address the issue of the relaxation term in the surface heat flux) and on the importance of the resolution of the ocean model on the modeling of the EMT: a switch from an eddy-permitting to an eddy-resolving model will allow us to estimate the importance of the mesoscale processes in the sequence of the EMT events.

[79] **Acknowledgments.** We thank Simon Josey and an anonymous reviewer for their very useful comments and discussions on this work. We acknowledge Philippe Rogel and Nicolas Daget from the CERFACS (Toulouse, France) for providing us the oceanic reanalysis data set used in the Atlantic zone. We also thank the NEMO Consortium and in particular the french laboratory "Laboratoire d'Océanographie et du Climat: Expérimentation et Approches Numériques" (LOCEAN, France). We thank Météo-France for the financial support of J. Beuvier's Ph.D. We are grateful to the European CIRCE project, for which the NEMOMED8 configuration was initially designed. This work will be continued in the frame of the SiMED national project on the modeling of the Mediterranean Sea at higher resolution and in the frame of the HyMeX international program on the study of the water cycle in the Mediterranean area.

References

Alhammoud, B., K. Béranger, L. Mortier, M. Crépon, and I. Dekeyser (2005), Surface circulation of the Levantine Basin: Comparison of model results with observations, *Prog. Oceanogr.*, *66*, 299–320.

Artegiani, A., D. Bregant, E. Paschini, N. Pinardi, F. Raicich, and A. Russo (1997), The Adriatic Sea general circulation. Part I: Air-Sea interactions and water mass structure, *J. Phys. Oceanogr.*, *27*, 1492–1514.

Barnier, B., L. Siefridt, and P. Marchesiello (1995), Thermal forcing for a global ocean circulation model using a three-year climatology of ECMWF analyses, *J. Mar. Syst.*, *6*, 363–380.

Barnier, B., et al. (2006), Impact of partial steps and momentum advection schemes in a global ocean circulation model at eddy-permitting resolution, *Ocean Dyn.*, *56*, 543–567.

Baschek, B., U. Send, J. Garcia Lafuente, and J. Candela (2001), Transport estimates in the Strait of Gibraltar with a tidal inverse model, *J. Geophys. Res.*, *112*, 31,033–31,044.

Béranger, K., L. Mortier, and M. Crépon (2005), Seasonal variability of water transport through the Straits of Gibraltar, Sicily and Corsica, derived from a high-resolution model of the Mediterranean circulation, *Prog. Oceanogr.*, *66*, 341–364.

Beuvier, J., F. Sevault, and S. Somot (2008), Modélisation de la variabilité interannuelle de la mer Méditerranée sur la période 1960–2000 à l'aide de NEMOMED8, *Note Cent. 105*, Groupe de Meteorol. de Grande Echelle et Clim., Cent. Natl. de Rech. Meteorol., Toulouse, France.

Blanke, B., and P. Delecluse (1993), Low frequency variability of the tropical Atlantic ocean simulated by a general circulation model with mixed layer physics, *J. Phys. Oceanogr.*, *23*, 1363–1388.

Bozec, A., P. Bouruet-Aubertot, K. Béranger, and M. Crépon (2006), Mediterranean oceanic response to the interannual variability of a

high-resolution atmospheric forcing: A focus on the Aegean Sea, *J. Geophys. Res.*, *111*, C11013, doi:10.1029/2005JC003427.
Bozec, A., P. Bouret-Aubertot, D. Iudicone, and M. Crépon (2008), Impact of penetrative solar radiation on the diagnosis of water mass transformation in the Mediterranean Sea, *J. Geophys. Res.*, *113*, C06012, doi:10.1029/2007JC004606.
Bryden, H. L. (1994), Exchange through the Strait of Gibraltar, *Prog. Oceanogr.*, *33*, 201–248.
Bryden, H. L., and T. H. Kinder (1991), Steady two-layer exchange through the Strait of Gibraltar, *Deep Sea Res.*, *38*, 445–463.
Canals, M., P. Puig, X. Durrieu de Madron, S. Heussner, A. Palanques, and J. Fabres (2006), Flushing submarine canyons, *Nature*, *444*, 354–357.
Candela, J. (2001), The Mediterranean water and the global circulation, in *Observing and Modelling the Global Ocean*, pp. 419–429, edited by G. Siedler, J. Church, and J. Gould, Academic, San Diego, Calif.
CLIPPER Project Team (1999), Modélisation à haute résolution de la circulation dans l'océan Atlantique forcée et couplée océan-atmosphére, *Sci. Tech. Rep. CLIPPER-R3-99*, Ifremer, Brest, France.
Daget, N., A. T. Weaver, and M. A. Balmaseda (2009), Ensemble estimation of background-error variances in a three-dimensional variational data assimilation system for the global ocean, *Q. J. R. Meteorol. Soc.*, *135*, 1071–1094.
Déqué, M., and J. Piedelievre (1995), High resolution climate simulation over Europe, *Cim. Dyn.*, *11*, 321–339.
Drillet, Y., R. Bourdallé-Badie, L. Siefridt, and C. Le Provost (2005), Meddies in the Mercator North Atlantic and Mediterranean Sea eddy-resolving model, *J. Geophys. Res.*, *110*, C03016, doi:10.1029/2003JC002170.
Gasparini, G. P., A. Ortona, G. Budillon, M. Astraldi, and E. Sansone (2005), The effect of the Eastern Mediterranean Transient on the hydrographic characteristics in the Strait of Sicily and in the Tyrrhenian Sea, *Deep Sea Res. Part I*, *52*, 915–935.
Gertman, I., N. Pinardi, Y. Popov, and A. Hecht (2006), Aegean Sea water masses during the early stages of the Eastern Mediterranean Climatic Transient (1988–90), *J. Phys. Oceanogr.*, *36*, 1841–1859.
Hamad, N., C. Millot, and I. Taupier-Letage (2005), A new hypothesis about the surface circulation in the eastern basin of the Mediterranean Sea, *Prog. Oceanogr.*, *66*, 287–298.
Herrmann, M., S. Somot, F. Sevault, C. Estournel, and M. Déqué (2008), Modeling the deep water convection in the northwestern Mediterranean Sea using an eddy-permitting and an eddy-resolving model: Case study of winter 1986–1987, *J. Geophys. Res.*, *113*, C04011, doi:10.1029/2006JC003991.
Herrmann, M. J., and S. Somot (2008), Relevance of ERA40 dynamical downscaling for modeling deep convection in the Mediterranean Sea, *Geophys. Res. Lett.*, *35*, L04607, doi:10.1029/2007GL032442.
Josey, S. A. (2003), Changes in the heat and freshwater forcing of the eastern Mediterranean and their influence on deep water formation, *J. Geophys. Res.*, *108*(C7), 3237, doi:10.1029/2003JC001778.
Klein, B., W. Roether, B. B. Manca, D. Bregant, V. Beitzel, V. Kovacevic, and A. Luchetta (1999), The large deep water transient in the eastern Mediterranean, *Deep Sea Res. Part I*, *46*, 371–414.
Klein, B., W. Roether, N. Kress, B. B. Manca, M. Ribera d'Alcala, E. Souvermezoglou, A. Theocharis, G. Civitarese, and A. Luchetta (2003), Accelerated oxygen consumption in eastern Mediterranean deep waters following the recent changes in thermohaline circulation, *J. Geophys. Res.*, *108*(C9), 8107, doi:10.1029/2002JC001454.
Kontoyiannis, H., E. Balopoulos, O. Gotsis-Skretas, A. Pavlidou, G. Assimakopoulou, and E. Papageorgiou (2005), The hydrodynamics and biochemistry of the Cretan Straits (Antikithira and Kassos straits) revisited in the period June 1997–May 1998, *J. Mar. Syst.*, *53*, 37–57.
Lascaratos, A. (1993), Estimation of deep and intermediate water mass formation rates in the Mediterranean Sea, *Deep Sea Res.*, *40*, 1327–1332.
Lascaratos, A., W. Roether, K. Nittis, and B. Klein (1999), Recent changes in deep water formation and spreading in the Eastern Mediterranean Sea: A review, *Prog. Oceanogr.*, *44*, 5–36.
Ludwig, W., E. Dumont, M. Meybeck, and S. Heussner (2009), River discharges of water and nutrients to the Mediterranean and Black Sea: Major drivers for ecosystem changes during past and future decades?, *Prog. Oceanogr.*, *80*, 199–217.
Macdonald, A. M., J. Candela, and H. L. Bryden (1994), An estimate of the net heat transport through the Strait of Gibraltar, in *Seasonal and Interannual Variability of the Western Mediterranean Sea Coastal and Estuarine Studies*, *Coastal Estuarine Stud. Ser.*, vol. 46, edited by P. E. La Violette, pp. 13–32, AGU, Washingtion, D. C.
Madec, G. (2008), NEMO ocean engine, *Note Pôle Model. 27*, Inst. Pierre-Simon Laplace des Sci. de l'Environ., Paris, France.
Madec, G., M. Delecluse, M. Imbard, and C. Levy (1998), OPA 8.1 Ocean General Circulation Model reference manual, *Note Pôle Model. 11*, 91 pp., Inst. Pierre-Simon Laplace des Sci. de l'Environ., Paris, France.
Malanotte-Rizzoli, P., B. B. Manca, M. Ribera d'Alcala, A. Thoecharis, S. Brenner, G. Budillon, and E. Ozsoy (1999), The eastern Mediterranean in the 80s and in the 90s: The big transition in the intermeditate and deep circulations, *Dyn. Atmos. Oceans*, *29*, 365–395.
MEDAR-MEDATLAS Group (2002), MEDAR/MEDATLAS 2002 database, Cruise inventory, observed and analysed data of temperature and bio-chemical parameters [CD-ROM], Ifremer, Brest, France.
Mertens, C., and F. Schott (1998), Interannual variability of deep-water formation in the northwestern Mediterranean, *J. Phys. Oceanogr.*, *28*, 1410–1424.
Millot, C. (1999), Circulation in the western Mediterranean Sea, *J. Mar. Syst.*, *20*, 423–442.
Nittis, K., A. Lascaratos, and A. Theocharis (2003), Dense water formation in the Aegean Sea: Numerical simulations during the Estern Mediterranean Transient, *J. Geophys. Res.*, *108*(C9), 8120, doi:10.1029/2002JC001352.
Oguz, T., and H. I. Sur (1989), A two-layer model of water exchange through the Dardanelles Strait, *Oceanol. Acta*, *12*, 23–31.
Reynaud, T., P. Legrand, H. Mercier, and B. Barnier (1998), A new analysis of hydrographic data in the Atlantic and its application to an inverse modeling study, *Int. WOCE Newsl.*, *32*, 29–31.
Rixen, M., et al. (2005), The Western Mediterranean Deep Water: A proxy for climate change, *Geophys. Res. Lett.*, *32*, L12608, doi:10.1029/2005GL022702.
Robinson, A. R., W. G. Leslie, A. Theocharis, and A. Lascaratos (2001), Mediterranean Sea Circulation, in *Encyclopedia of Ocean Sciences*, edited by J. H. Steele, S. A. Thorpe, and K. K. Turekian, pp. 1689–1706, Academic, London.
Roether, W., B. B. Manca, B. Klein, D. Bregant, D. Georgopoulos, V. Beitzel, V. Kovacevic, and A. Luchetta (1996), Recent changes in Eastern Mediterranean Deep Waters, *Science*, *271*, 333–335.
Roether, W., B. Klein, B. B. Manca, A. Theocharis, and S. Kioroglou (2007), Transient Eastern Mediterranean Deep Waters in response to the massive dense-water output of the Aegean Sea in the 1990s, *Prog. Oceanogr.*, *74*, 540–571.
Roullet, G., and G. Madec (2000), Salt conservation, free surface, and varying levels: A new formulation for ocean general circulation models, *J. Geophys. Res.*, *105*, 23,927–23,942.
Rupolo, V., S. Marullo, and D. Iudicone (2003), Eastern Mediterranean Transient studied with Lagrangian diagnostics applied to a Mediterranean OGCM forced by satellite SST and ECMWF wind stress for the years 1988–1993, *J. Geophys. Res.*, *108*(C9), 8121, doi:10.1029/2002JC001403.
Samuel, S., K. Haines, S. Josey, and P. G. Myers (1999), Response of the Mediterranean Sea thermohaline circulation to observed changes in the winter wind stress field in the period 1980–1993, *J. Geophys. Res.*, *104*, 7771–7784.
Schroeder, K., A. Ribotti, M. Borghini, R. Sorgente, A. Perilli, and G. P. Gasparini (2008), An extensive Western Mediterranean Deep Water renewal between 2004 and 2006, *Geophys. Res. Lett.*, *35*, L18605, doi:10.1029/2008GL035146.
Sevault, F., S. Somot, and J. Beuvier (2009), A regional version of the NEMO ocean engine on the Mediterranean Sea: NEMOMED8 user's guide, *Note Cent. 107*, Groupe de Meteorol. de Grande Echelle et Clim., Cent. Natl. de Rech. Meteorol., Toulouse, France.
Simmons, A., and J. Gibson (2000), The ERA40 project plan, *ERA40 Proj. Rep. 1*, Eur. Cent. for Medium-Range Weather Forecasts, Reading, U. K.
Smith, W. H. F., and D. T. Sandwell (1997), Global sea floor topography from satellite altimetry and ship depth sounding, *Science*, *277*, 1956–1962.
Somot, S. (2005), Modélisation climatique du bassin méditerranéen: Variabilité et scénarios de changement climatique, Ph.D. thesis, Spec. Phys. du Clim., Univ. de Toulouse III Paul Sabatier, Toulouse, France.
Somot, S., and J. Colin (2008), First step towards a multi-decadal high-resolution Mediterranean Sea reanalysis using dynamical downscaling of ERA40, Research activities in atmospheric and oceanic modelling, *Rep. 38*, World Meteorol. Organ., Geneva, Switzerland.
Somot, S., F. Sevault, and M. Déqué (2006), Transient climate change scenario simulation of the Mediterranean Sea for the twenty-first century using a high-resolution ocean circulation model, *Clim. Dyn.*, *27*, 851–879.
Sotillo, M. G., A. W. Ratsimandresey, J. C. Carretero, A. Bentamy, F. Valero, and F. González-Rouco (2005), A high-resolution 44-year atmospheric hindcast for the Mediterranean Basin: Contribution to the regional improvement of global reanalysis, *Clim. Dyn.*, *25*, 219–236.
Stanev, E. V., and E. L. Peneva (2002), Regional sea level response to global climatic change: Black Sea examples, *Global Planet. Changes*, *32*, 33–47.
Stanev, E. V., P.-Y. Le Traon, and E. L. Peneva (2000), Sea level variations and their dependancy on meteolorogical and hydrological forcing:

Analysis of altimeter and surface data for the Black Sea, *J. Geophys. Res.*, *105*, 17,203–17,216.
Stratford, K., and K. Haines (2000), Frictional sinking of the dense water overflow in a z-coordinate OGCM of the Mediterranean Sea, *Geophys. Res. Lett.*, *27*, 3969–3972.
Sur, H. I., E. Ozsoy, and U. Unluata (1992), Simultaneous deep and intermediate depth convection in the northern Levantine Sea, winter 1992, *Oceanol. Acta*, *16*, 33–43.
Theocharis, A., and H. Kontoyiannis (1999), Interannual variability of the circulation and hydrography in the eastern Mediterranean (1986–1995), in *The Eastern Mediterranean as a Laboratory Basin for the Assessment of Contrasting Ecosystems*, *NATO Sci. Ser.: 2. Environ. Security*, vol. 51, edited by P. Malanotte-Rizzoli and V. N. Eremeev, pp. 453–464, Kluwer Acad., Dordrecht, Netherlands.
Theocharis, A., K. Nittis, H. Kontoyiannis, E. Papageorgiou, and E. Balopoulos (1999), Climatic changes in the Agean Sea influence the eastern Mediterranean thermohaline circulation (1986–1997), *Geophys. Res. Lett.*, *26*, 1617–1620.
Theocharis, A., B. Klein, L. Nittis, and W. Roether (2002), Evolution and status of the Eastern Mediterranean Transient (1997–1999), *J. Mar. Syst.*, *33–34*, 91–116.
Tsimplis, M., M. Marcos, S. Somot, and B. Barnier (2008), Sea level forcing in the Mediterranean Sea between 1960 and 2000, *Global Planet. Change*, *63*, 325–332.
Tsimplis, M., M. Marcos, J. Colin, S. Somot, A. Pascual, and A. G. P. Shaw (2009), Sea level variability in the Mediterranean Sea during the 1990s on the basis of one 2D and one 3D model, *J. Mar. Syst.*, *78*, 109–123.
Tsimplis, M. N., and H. L. Bryden (2000), Estimation of the transport through the Strait of Gibraltar, *Deep Sea Res. Part I*, *47*, 2219–2242.
Tsimplis, M. N., and S. A. Josey (2001), Forcing of the Mediterranean Sea level by atmospheric oscillations over the North Atlantic, *Geophys. Res. Lett.*, *28*, 803–806.
Von Storch, H., H. Langeberg, and F. Feser (2000), A Spectral Nudging Technique for Dynamical Downscaling Purposes, *Mon. Weather Rev.*, *128*, 3664–3673.
Vörösmarty, C., B. Fekete, and B. Tucker (1996), Global River Discharge Database, RivDis, http://www.rivdis.sr.unh.edu/, U. N. Educ. Sci. and Cult. Organ., Paris.
Wijffels, S. E., J. Willis, C. M. Domingues, P. Barker, N. J. White, A. Gronell, K. Ridgway, and J. A. Church (2008), Changing expendable bathythermograph fall-rates and their impact on estimates of thermosteric sea level rise, *J. Clim.*, *21*, 5657–5672.
Wu, P., K. Haines, and N. Pinardi (2000), Toward an understanding of deep-water renewal in the eastern Mediterranean, *J. Phys. Oceanogr.*, *30*, 443–458.
Wüst, G. (1961), On the vertical circulation of the Mediterranean Sea, *J. Geophys. Res.*, *66*, 3261–3271.
Zervakis, V., D. Georgopoulos, and P. G. Drakopoulos (2000), The role of the North Aegean in triggering the recent eastern Mediterranean climatic changes, *J. Geophys. Res.*, *105*, 26,103–26,116.
Zervakis, V., D. Georgopoulos, A. Karageorgis, and A. Theocharis (2004), On the response of the Aegean Sea to climatic variability: A review, *Int. J. Climatol.*, *24*, 1845–1858.

K. Béranger and J. Beuvier, Unité de Mécanique, Ecole Nationale Supérieure de Techniques Avancées, ParisTech, Chemin de la Hunière, F-91761 Palaiseau, France. (jonathan.beuvier@ensta.fr)
M. Herrmann, F. Sevault, and S. Somot, Groupe d'Etude de l'Atmosphère Météorologique, Centre National de Recherches Météorologiques, Météo-France, CNRS, 42 Ave. Gaspard Coriolis, F-31057 Toulouse CEDEX 1, France.
H. Kontoyiannis, Institute of Oceanography, Hellenic Center for Marine Research, Aghios Kosmas, GR-16604 Athens, Greece.
W. Ludwig, Centre de Formation et de Recherche sur l'Environnement Marin, Université de Perpignan, 52 Ave. Paul Alduy, F-66860 Perpignan, France.
M. Rixen, NATO Undersea Research Centre, Viale San Bartolomeo 400, I-19138 La Spezia, Italy.
E. Stanev, Institute for Coastal Research, GKSS Research Center, Max-Planck-Str. 1, D-21502 Geesthacht, Germany.